Functional Studies of Penicillin-binding Protein 1 in *Bacillus subtilis*

Lin Liu

Thesis submitted to the faculty of the Virginia Polytechnic Institute and State University in partial fulfillment of the requirements for the degree of

Master of Science

in

Biological Sciences

Committee members:

Chair: David L. Popham

Ann M. Stevens

Brenda S. J. Winkel

Tim Larson

Zhaomin Yang

April 30, 2007

Blacksburg, VA

Keywords: *Bacillus subtilis*, penicillin-binding proteins (PBPs), phenotype, localization

Functional Studies of Penicillin-binding Protein 1 in *Bacillus subtilis*

Lin Liu
David L. Popham, Chair
Department of Biological Sciences, Virginia Polytechnic Institute and State University

ABSTRACT

The penicillin-binding proteins (PBPs) synthesize and modify peptidoglycan (PG), the main structural element of the bacterial cell wall. PBPs and PG synthesis are highly conserved in all bacteria and both have been important targets for antibiotic and antibacterial development. In the Gram positive bacterium *Bacillus subtilis*, PBP1 is composed of the four domains S, N, P, and C in order from the N- to C-terminus. It plays important roles in vegetative PG synthesis. Compared to the wild type *B. subtilis*, the PBP1 null mutant has decreased growth rate, cell diameter, and PG crosslinking; the cell population has more long cells; and the colonies have raised and smooth edges. In this work, we constructed six mutant forms of PBP1 that were tagged with a C-terminal FLAG epitope, to complement the wild type gene. We examined the colony and cell morphologies, and PBP1 localization in the mutant strains. The removal of the cytoplasmic region of the PBP1 S domain and the replacement of PBP1 S domain by PBP4 S domain did not change the colony morphologies, and each of these two mutations had minor effects on growth rate, cell diameter, PG crosslinking and generation of long cells in the cell population. The single point mutation in the active site of the N or P domain presumably removed the enzymatic activity, and each mutation caused slower growth rate, decreased cell diameter and PG crosslinking. The point mutation in the P domain had a minor effect on the colony morphology and formation of long cells; while the mutation in the N domain altered the colony morphology, and resulted in high percentage of long cells that is comparable to the PBP1 null mutant. The C domain of PBP1 has no apparent enzymatic activity, but the loss of it altered the colony morphology, and caused slower growth rate, decreased cell diameter, and PG crosslinking. In the wild type *B. subtilis*, PBP1 localizes to the septum. This septum localization specificity was lost in strains expressing PBP1 without the C domain, with PBP4 S domain, or with a point mutation in the

active site of the N domain. PBP1 with a point mutation in the active site of the P domain, or without the cytoplasmic region of the S domain, had decreased septum localization specificity. These findings were used to develop a model of how PBP1 domain functioning in *B. subtilis.*

ACKNOWLEDGEMENTS

I came to America following my dreams for open minded and competitive research, and had it realized gradually in the Popham's lab. I am thankful to the hospitality of Virginia Tech., and it made the years of studying and living in Blacksburg a wonderful experience. I am especially grateful to the accompaniment of many people.

Thanks to my supervisor, Dr. David L. Popham. I could not stand at where I am today without your patient teaching and guidance. Your influence will last after my graduation.

Thanks to Dr. Ann M. Stevens, Dr. Brenda S. J. Winkel, Dr. Tim Larson and Dr. Zhaomin Yang, for the advice and encouragement throughout the years.

Thanks to Michelle Dickens, Jessica McElligott, Benjamin Orsburn, Yong Xue, Pradeep Vasudevan, Emily Plass, Jared Heffron, and past labmates for help and making the lab enjoyable.

Thanks to all other labs in the micro group. Daniel Schu, Zhuo Li, Qian Xu, Xiaohui Cui and many others, graduate life with you was a lot more smooth and happy.

Thanks to Nan Qin, my dear husband and wise colleague, for all the love and support.

LIST OF FIGURES

LIST OF TABLES

TABLE OF CONTENTS

REVIEW OF LITERATURE

Bacterial Cell Wall and Peptidoglycan Structure

The bacterial cell wall is required to maintain cell shape and to protect cells from osmotic lysis. Peptidoglycan (PG) is the main structural component of the bacterial cell wall. It is consists of glycan strands with alternating units of N-acetyl muramic acid (NAM) and N-acetylglucosamine linked by beta-1,4 glucosidic bonds, with adjacent glycan strands cross-linked by short peptides attached to NAM residues (Figure 1) (Foster 2001). PG can differ among species in several respects: the length of glycan strands can vary from 10 dissacharide units in the Gram negative bacterium *Escherichia coli* to approximately 100 dissacharide units in the Gram positive bacterium *Bacillus subtilis* (Ward 1973). The peptide side chains are often composed of L-alanine-D-glutamate-meso-diaminopimelic acid (Dpm)-D-alanine-D-alanine, as in *B. subtilis* and *E. coli* (Archibald 1993), but they can contain other amino acids (Schleifer and Kandler 1972). There can be peptide cross-bridges involved in cross-linking between the peptide side-chains, and there can be acetylation and deacetylation of the glycan strands (Archibald 1993). Gram positive bacteria have large amounts of anionic teichoic acids attached to NAM residues, which may function to slow diffusion of some molecules towards or away from the cytoplasmic membrane, acting similarly to the outer cell membrane in Gram negative bacteria (Archibald, Armstrong et al. 1961; Archibald 1993). The PG layer is 20 times thinner in Gram negative bacteria than in Gram positive bacteria. Although the PG composition varies in different species, the gross PG structure and the PG synthesis mechanism is highly conserved in all bacteria.

PG synthesis and PBP functions

PG in the vegetative cell has a dynamic structure. It is continuously being synthesized, modified and hydrolyzed to allow for cell growth and division. During PG synthesis, the precursors UDP-NAG and UDP-NAM are synthesized in the cytoplasm,

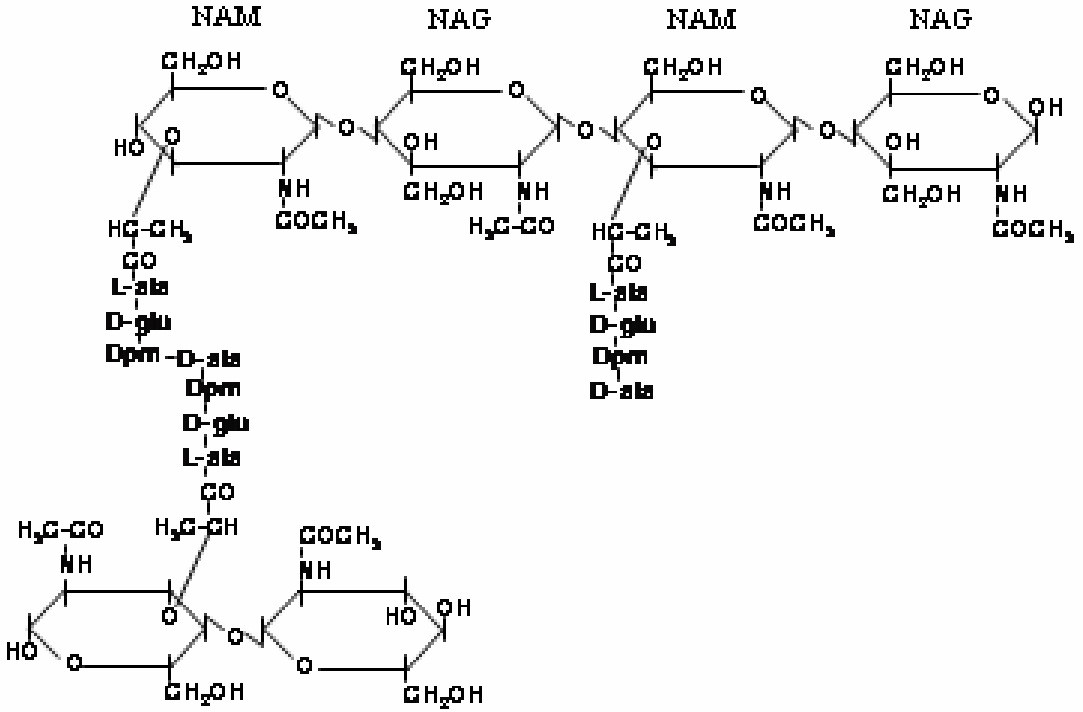

Figure 1. Typical peptidoglycan structures of bacteria. Peptidoglycan is composed of glycan chains with alternating units of NAM (N-acetyl muramic acid) and NAG (N-acetyl glucosamine) with crosslinked peptides attached to NAM. Composition of peptide side chains varies in different species.

followed by step-wise addition of amino acids (Meadow, Anderson et al. 1964) to NAM residues to form the UDP-NAM-pentapeptides. UMP is then removed and the P-NAM-pentapeptide is linked to a membrane C_{55}-undecaprenol lipid carrier (Higashi, Strominger et al. 1967) to form the NAM (pentapeptide)-PP-Lipid known as Lipid I. The UDP-NAG precursor is added to Lipid I in a reaction with removal of UDP and formation of a beta-1, 4 glycosidic bond with NAM. The synthesized NAG-NAM (pentapeptide)-PP-Lipid is called Lipid II. In the second stage, the Lipid II precursors are flipped across the cytoplasmic membrane (Anderson, Meadow et al. 1966; Archibald 1993). During the final steps of PG synthesis, to polymerize the glycan strands and utilize the peptide side-chains to cross-link the PG network, the required enzymatic activities are glycosyl transferase (GT) and transpeptidase (TP), respectively. Catalyzed by GT, disaccharide units of Lipid II are added to the growing glycan chains by forming beta-1, 4 glycosidic bonds between them in a reaction involving removal of a H_2O molecule (Figure 2). TP removes the terminal alanine from a peptide side chain, and cross-links that side chain with the Dpm of a peptide side chain on an adjacent glycan strand (Figure 2). Additional activities can further modify the peptide side chains. Endopeptidases can cleave the cross-linking peptides to di- or tri- peptides. Carboxypeptidases cleave the uncross-linked pentapeptides to tetra- or tri- peptides, thus blocking further cross-linking. All of these enzymatic activities that play most important roles in bacterial cell wall PG synthesis are associated with penicillin-binding proteins (PBPs) (Archibald 1993).

Beta-lactam antibiotics and penicillin-resistance

PBPs have been a focus of antibacterial research since the discovery of penicillin because of their essential roles in PG synthesis, without which bacterial cells can not survive. The broad spectrum activity of anti-PBP antibiotics is due to the conserved PG structure and synthesis mechanism in all bacteria. The importance of this is reflected in the large number of antibiotics targeting PBPs that are widely used for antibacterial therapy.

Penicillin belongs to a class of antibiotics that share a three-carbon, one-nitrogen

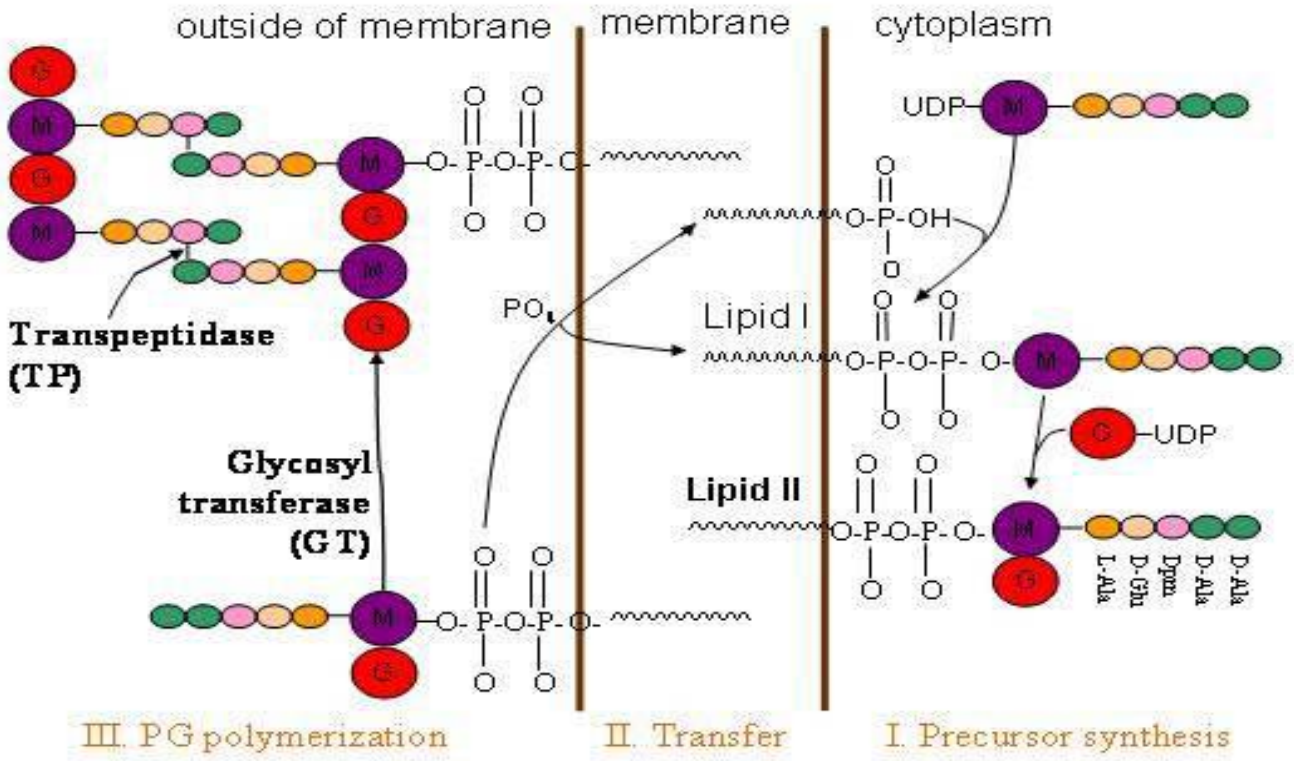

Figure 2. PG synthesis. In the first stage, Lipid II precursors are synthesized in the cytoplasm. In the second stage, Lipid II is transferred to the outside of cell membrane. In the third stage, disaccharides are added to the growing glycan chains, catalyzed by glycosyl transferase, and the peptide side chains are cross-linked by transpeptidase.

four-atom structure known as the beta-lactam ring. Beta-lactam antibiotics can bind and inactivate PBPs. The characteristic ring mimics the D-ala-D-ala moiety of the PG structure, so it can be recognized by and bind to the serine in the active cleft of PBPs (Tipper and Strominger 1965). The resulting acyl complex is very stable and the PBPs can not be released to function. Beta-lactamases undergo the same reaction, but can rapidly deacylate the beta-lactam-protein complex and hydrolyze the beta-lactam antibiotic (Ghuysen 1991).

Bacteria can acquire beta-lactam resistance through several mechanisms: 1) variation of the target proteins (PBPs) to decrease their affinity to bind antibiotics, 2) expression of efflux pumps to reduce drug permeation across the outer membrane, 3) modification of the PBP complement or function in the cell, and 4) production of beta-lactamase enzymes (Hakenbeck and Coyette 1998). The genes coding for beta-lactamases can be located on the bacterial chromosome or on transmissible plasmids (Williams 1999). In the Gram negative bacteria, beta-lactamases are exported to the periplasm and in the Gram positive bacteria beta-lactamases are secreted outside of cells (Rice, Carias et al. 2001).

PBP classes and domains

PBPs are grouped into three classes based on molecular weight (MW) and conserved amino acid motifs (Figure 3) (Ghuysen 1991; Goffin and Ghuysen 1998). Class A and Class B PBPs are high MW (≥ 60kD) PBPs, and have four domains: S, N, P and C, in this order from the N- to C-terminus. The S domain contains a cytoplasmic region plus an uncleaved signal peptide that forms a single helix crossing the membrane and serves as a membrane anchor. The C domain is a C-terminal tail of highly variable length and sequence, with no defined function. However, the C domain of PBP2b, a Class B PBP in *B. subtilis*, is required for maintaining the wild type cellular phenotype, suggesting its role in protein interactions or stability (Yanouri, Daniel et al. 1993). The N domain of Class A and Class B PBPs are not related in terms of either sequence or function (Goffin and Ghuysen 1998). The N domain of Class A PBPs have six conserved

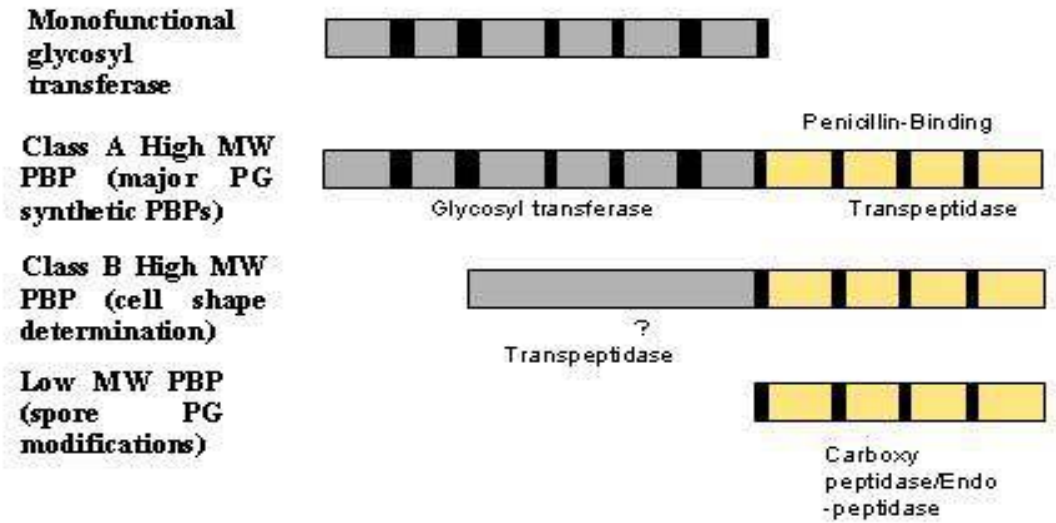

Figure 3. PBP classes and domains. Black blocks represent highly conserved sequences. The six conserved motifs in the GT domain of class A PBPs and MGTs are shown. All PBPs share a penicillin-binding domain. Three conserved sequences form the site targeted by penicillin, which is also the active site for transpeptidase activity.

motifs that are part of the active site for GT enzymatic activity (Goffin and Ghuysen 1998). These six conserved motifs are also found in monofunctional GT proteins (MGTs) (Goffin and Ghuysen 1998) that exist in some organisms such as *E. coli* and *Streptococcus pneumoniae* but not in *B. subtilis*. This domain is the target for moenomycin-type antibiotics, which inhibit GT by mimicking the substrate structure (Welzel 1993). Class A PBPs are believed to be the only PBPs with GT enzymatic activity.

The N domain of Class B PBPs contains four conserved motifs (Goffin and Ghuysen 1998). The N domain in Class B PBPs aids in the correct folding to maintain functional conformation (Goffin and Ghuysen 1998). Once there was a suggestion that class B PBPs had GT activity (Ishino and Matsuhashi 1981), but it could not be proved and the function of this N domain remains unclear (Adam, Fraipont et al. 1997; van Heijenoort, Gomez et al. 1992).

All PBPs share three highly conserved motifs in their P domains (Goffin and Ghuysen 1998), which act as the active site for TP activity in high MW PBPs or for endo- and carboxy-peptidase activity in low MW PBPs. They are also the target sites for the beta-lactam antibiotics such as penicillin. Mutations in or adjacent to the active site can affect the sensitivity of PBPs to beta-lactams (Gerrits, Godoy et al. 2006; Smith and Klugman 2005).

Low MW PBPs (≤ 60kD) and single domains of PBPs have been crystallized and their structures studied (Nicholas, Krings et al. 2003; Sauvage, Kerff et al. 2002). Recent studies of a soluble form of high MW PBP1b (lacking most of the GT domain) of *S. pneumoniae* give insight into the folding of full length high MW PBP (Macheboeuf, Di Guilmi et al. 2005). With the aid of the 3D structures of PBPs, interactions with new drugs and other proteins can be predicted prior to laboratory investigation.

***B. subtilis* PBPs and their phenotypic effects**

Class A PBPs are the only bifunctional PBPs with both GT and TP functions. Genetic studies have shown that these proteins play major roles in vegetative PG synthesis.

Four Class A PBPs have been identified through sequence analysis in *B. subtilis*: PBP1, PBP4, PBP2c, and PBP2d, encoded by *ponA* (Popham and Setlow 1995), *pbpD* (Popham and Setlow 1994), *pbpF,* (Popham and Setlow 1993) and *pbpG* (Pedersen, Ragkousi et al. 2000), respectively.

PBP1 is the most abundant Class A PBP in log phase vegetative cells (Popham and Setlow 1996). It plays major roles in vegetative PG synthesis. The doubling time of *ponA* null mutants increases from 20 minutes in the wild type to 28 minutes (Popham and Setlow 1995) or 25 minutes (McPherson and Popham 2003) in rich medium. The cell diameter decreases about 16% (Popham and Setlow 1995). In the *ponA* mutant cell population there are more long cells, with some defect in the formation of division patterns, and some of the cells are slightly bent (Popham and Setlow 1996). The crosslinking of the peptide side chains in the PG structure in log-phase cells decreases from 26% in the wild type, to 24% in the *ponA* null mutant (McPherson and Popham 2003). The sporulation efficiency decreases significantly from 100% to 14% (Popham and Setlow 1996). The nutrients are most limited at the center of colonies, and the raised, winkled center of wild type colonies presumably indicates the formation of spores. PBP1 null mutants have flat-center colonies (Popham and Setlow 1995), consistent with the sporulation defect relative to the wild type (Popham and Setlow 1995). PBP1 function can be partially compensated for by other Class A PBPs (PBPs 4 and 2c) (Popham and Setlow 1996).

PBP4 is the shortest and least complex of the Class A PBPs and has a minor role in vegetative PG synthesis. It can partially compensate for the PBP1 functions (Popham and Setlow 1996). A *pbpD* single mutant does not show obvious phenotypic changes, but a *ponA pbpD* double mutant has phenotypic changes greater than *ponA* single null mutant. The other two members of the Class A PBPs, PBP2c and PBP2d, play redundant roles in spore germ cell wall PG synthesis and minor roles in vegetative PG synthesis (McPherson, Driks et al. 2001; Popham and Setlow 1996). Class A PBPs and MGTs were thought to be

the only proteins conferring GT activity, thus playing indispensable and partially redundant roles in PG synthesis. Yet it must be noted that *B. subtilis* has no MGTs and can survive when all four Class A PBPs are absent, which indicates the presence of one or more other proteins with GT activity (McPherson and Popham 2003). The identity of this GT has not been determined.

The Gram positive bacterium *Streptococcus pneumoniae* has three Class A high MW PBPs: PBPs 1a, 1b, and 2a (Table 1). Single null mutations of these PBPs have no or minor effects on cell phenotype (Hoskins, Matsushima et al. 1999), but a PBP1a-, 2a- double mutant was non-viable (Hoskins, Matsushima et al. 1999). So the presence of either PBP1a or 2a is essential for cell growth. Another Gram positive bacterium, *Staphylococcus aureus,* has four PBPs (PBPs 1 to 4). PBP2 is the only bifunctional Class A PBP, and its TP activity is required for cell viability (Pinho, Filipe et al. 2001). The other three PBPs have only transpeptidase activity (Pinho, de Lencastre et al. 2000; Wada and Watanabe 1998; Wyke, Ward et al. 1981). *E. coli* has twelve known PBPs. PBPs 1a, 1b and 1c are high MW Class A PBPs. PBPs 1a-, 1b- double null mutants are not viable so the presence of at least one of these PBPs is indispensable for cell growth (Denome, Elf et al. 1999). Removal of a single or combination of Class A PBPs (except PBPs 1a/1b double null mutation) in *E. coli* generated little phenotypic change (Schiffer and Holtje 1999; Yousif, Broome-Smith et al. 1985). Cells with single or multiple null mutations (all possible combinations except a PBPs 1a/1b double null mutation) of eight PBPs (Class A PBPs 1a, 1b and low MW PBPs 4, 5, 6, 7, AmpC and AmpH) are all viable (Denome, Elf et al. 1999). *E. coli* and *S. pneumoniae* each has one monoglycosyl transferase (MGT).

Class B PBPs are mono-functional PBPs with only TP activity in their P domain, and are important in cell shape determination. In *B. subtilis*, there are six Class B PBPs, PBP2a, PBP2b, PBP3, PBP4b (also known as YrrR), PBPH (also known as YkuA), and SpoVD, encoded by *pbpA*, *pbpB*, *pbpC*, *pbpI*, *pbpH*, and *spoVD*, respectively. PBP2a and PBPH function in cylindrical wall PG cross-linking and are associated with cell wall

Table 1. Class A and Class B PBPs in several model bacteria. *E. coli* is Gram negative bacterium. *B. subtilis, S. pneumoniae* and *S. aureus* are Gram positive species.

Bacterium	Class A PBPs	Class B PBPs
Bacillus subtilis	1, 4, 2c, 2d	2a, 2b, 3, 4b, PBPH, SpoVD
Streptococcus pneumoniae	1a, 1b, 2a	2b, 2x
Staphylococcus aureus	2	1, 3, 4
Escherichiae coli	1a, 1b, 1c	2, 3

elongation (Wei, Havasy et al. 2003). PBP2b's activity is essential in septal PG cross-linking (Daniel, Harry et al. 2000). SpoVD functions in spore cortex PG cross-linking (Daniel, Drake et al. 1994). PBP3 was found to be dispensable alone or in combination with other PBPs (Murray, Popham et al. 1996). PBP4b is specifically expressed in the forespore, but its function is unclear (Wei, McPherson et al. 2004).

Low MW PBPs are single domain, mono-functional PBPs. PBP5, the product of *dacA*, is the most abundant PBP in vegetative cells, and its amount remains significant in sporulation (Sowell and Buchanan 1983). As a carboxypeptidase, it can cleave the peptide side chains to tripeptides. Mutants lacking PBP5 change PG structure greatly in that the pentapeptide side-chains increase about 30 times relative to the wide type strain (Popham, Helin et al. 1996). However, the mutants have PG cross-linking, growth rate, and cell phenotype similar to the wild type cells (Todd, Roberts et al. 1986). PBP5* (encoded by *dacB*) (Buchanan and Ling 1992) and DacF (encoded by *dacF*) (Wu, Schuch et al. 1992) function as carboxypeptidases and play partially redundant roles in regulating the cross-linking level of spore PG (Popham, Gilmore et al. 1999).

Bacterial cell shape determination

Characteristic cell shape has long been a critical criterion for classifying bacterial species. The examples can be streptococci (coccus or spherical), bacilli (rod-shaped) and spirochaetes (spiral). This cell shape is determined by the PG structure outside of the cell. PG synthetic and remodeling-proteins, including PBPs, RodA (Henriques, Glaser et al. 1998), Min (Reeve, Mendelson et al. 1973), and Fts (Vicente, Rico et al. 2006) proteins, can affect the cell shape. Genes involved in the synthesis of teichoic acids in Gram positive cells are also cell shape determinants. In recent years, research has shown that bacteria have actin-like proteins MreB and Mbl. They form distinct helical patterns as a cytoskeleton underneath the cell membrane, and mutations in these genes affect the cell shape (Cabeen and Jacobs-Wagner 2005; Stewart 2005). In *B. subtilis*, MreB is essential in rich medium. However, at high magnesium concentrations MreB is not essential and cell

morphology of the mutant is similar to that of the wild type (Formstone and Errington 2005). In the early stage of MreB depletion cells become spheres and chromosome segregation is affected (Defeu Soufo and Graumann 2005), suggesting its role in regulating cell shape (Jones, Carballido-Lopez et al. 2001). MreB is not essential in *E. coli*, but forms a similar helical structure as in *B. subtilis*. Mbl null mutant cells are bent and twisted, and it was proposed to determine the cell diameter (Jones, Carballido-Lopez et al. 2001). Mbl filaments and nascent cell wall synthesis occur in identical helical patterns in *B. subtilis*, and in a *mbl* null mutant the PG precursor pattern on the side walls of cells disappears, which suggests that Mbl and PG synthesis cooperate to determine the cell shape (Daniel and Errington 2003). However, this result could not be repeated in another lab. Instead, it was shown that a *mbl* null mutation did not affect the nascent PG insertion sites (Tiyanont, Doan et al. 2006). Moreover, *mbl* null mutants appear to have an unclosed FtsZ ring (Jones, Carballido-Lopez et al. 2001). MreB interacts with the membrane proteins MreCD (Kruse, Bork-Jensen et al. 2005). In *Caulobacter crescentus* MreC interacts with both MreB and several PBPs (Divakaruni, Loo et al. 2005). Based on these findings a model has been proposed for how PBPs, MreBCD, and Mbl function cooperatively to determine cell shape in *B. subtilis* (Stewart 2005) (Figure 4). In this model MreB and Mbl each forms distinct helices along the cell axis and contacts the cell membrane via the MreCD complex. The MreCD complex is further proposed to interact with the PBPs that synthesize cell wall PG.

Divisomes, PBP localization, and PBP-protein interactions

In Gram negative bacteria such as *E. coli*, PBP1 is part of the cell divisome and the recruitment order of proteins to form this complex is essentially strict (Vicente, Rico et al. 2006). The divisome complex contains at least 15 proteins including cytoplasmic, membrane, and periplasmic proteins. Through localization studies the recruitment order was roughly identified as an almost linear pathway: FtsZ > [FtsA, ZapA, ZipA] > FtsE/X > FtsK > FtsQ > FtsB/L > FtsW >FtsI > FtsN (Vicente, Rico et al. 2006). Proteins in

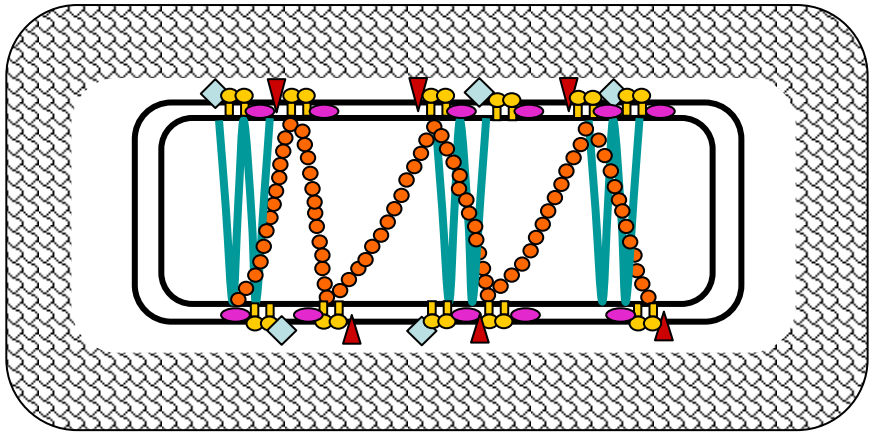

Figure 4. Model for the involvement of MreB and Mbl in bacterial cell wall synthesis in *Bacillus subtilis*. Proposed by Dr. Stwart, MreB (green) and Mbl (orange) helices contact cell membrane at MreCD. MreCD interact with PBPs which catalyze PG synthesis. MreD proteins are depicted as pink ovals, MreC dimers in yellow, PBP2b as green diamonds, and other PBPs in red. PBP2b localizes at mid-cell and potential division sites.

brackets localize independently of each other. Some recent research used a premature-targeting method and localized proteins to the Z-ring by fusion to the FtsZ-binding protein ZapA, then studied the localization of other divisome proteins following selective depletion of upstream proteins (Goehring, Gonzalez et al. 2006; Goehring, Gueiros-Filho et al. 2005). These studies showed that the recruitment of most proteins to the division sites can be independent of the upstream proteins and their presences instead can back-recruit upstream proteins (Goehring, Gonzalez et al. 2006). A revised divisome model was proposed (Goehring, Gonzalez et al. 2006). In this model, at least three complexes are involved in the divisome: a Z-ring complex, a Fts Q/L/B complex, and a PG synthetic complex. In the Gram positive bacterium *B. subtilis*, localization studies showed that the divisome seems to have a concerted or cooperative mode of protein recruitment, rather than a linear sequence, and the reason for this may lie in the different cell wall nature and division mechanisms. Septum formation and constriction in *E. coli* happen simultaneously and the thin (one or two) layers of PG require a tight regulation by enzymes for maintenance; in *B. subtilis* constriction follows septum formation, and the PG layers are about 20 times thicker than those in *E. coli*.

Recent studies of PBP localization using fluorescence microscopy have further enhanced the understanding of cell wall synthesis. In vegetative growth of *B. subtilis*, PBP1 localizes to the septum (Pedersen, Angert et al. 1999) and the localization depends on several division proteins. So PBP1 can be considered a part of the cell division machinery (Scheffers and Errington 2004), but no evidence of direct protein interactions is available. PBP2b also localizes at the septum, and this agrees with the protein's function in septal PG cross-linking (Daniel, Harry et al. 2000). PBPs 3 and 4a specifically localize to the lateral wall in vegetative *B. subtilis*, in distinct foci (Scheffers and Errington 2004), and this suggests space-specific rather than dispersed PG synthesis. Other PBPs localize both to the septum and to the lateral cell wall (Scheffers, Jones et al. 2004). During asymmetric sporulation, PBPs 2c and 2d locate at the prespore septum and follow the

mother cell membrane during engulfment (Scheffers 2005). PBPx, as an endopeptidase, changes its location and forms a spiral pattern similar to that of FtsZ, FtsA and EzrA during sporulation (Scheffers 2005).

PG synthesis, modification, and degradation must be well regulated to maintain a stable and functional cell wall. PBPs and autolysins may exist as a complex in Gram negative bacteria during PG synthesis for cell septation and elongation (Alaedini and Day 1999). Recent study reveals a direct interaction between a Class A PBP (PBP1b) and a Class B PBP (PBP3) in *E. coli* (Bertsche, Kast et al. 2006). No evidence of direct PBP-protein interactions has been demonstrated in Gram positive bacteria. But some facts suggest the existence of cooperation among PBPs, and they may function together with some other cell-shape-determinant proteins as a complex. In *B. subtilis* PBP1 localizes to the vegetative septum and is part of cell division machinery (Scheffers and Errington 2004). PBP2b also specifically localizes at the septum (Scheffers, Jones et al. 2004). Several PBPs have been shown to be co-located at septal sites during Stage II of the sporulation process (Rubio and Pogliano 2004). Other indirect evidence for PBP1-involved cooperation is that *B. subtilis* forms an increasing gradient of cross-linking from the inside to the outside of PG (Meador-Parton and Popham 2000). A thorough study on PBP-protein interactions is needed to clarify how PBPs function to produce a stable and reproducible cell shape.

The work presented here is focused on functional studies of *B. subtilis* PBP1 domains. PBP1 affects growth rate, cell length, cell diameter, and colony morphology, and PBP1 localizes to the septum. By studying the phenotypic effects and localization of six mutant forms of PBP1, we aimed to determine the functions of specific PBP1 domains and the activities required for certain PBP and cell properties.

MATERIALS AND METHODS

Bacterial strains and growth medium

All *B. subtilis* strains were derivatives of strain 168 and are listed in Table 2. *B. subtilis* was naturally transformed as previously described (Anagnostopoulos and Spizizen 1961). Growth was at 37ºC in 2xSG (Leighton and Doi 1971) for *B. subtilis*, and in 2xYT (Popham and Setlow 1996) for *E. coli*, containing appropriate antibiotics: chloramphenicol (3 μg/ml), spectinomycin (100 μg/ml), ampicillin (50μg/ml). In agar medium 40 μg/ml IPTG and 10 μg/ml X-gal were added to screen *E. coli* transformants, and 1% starch was added for amylase activity examination. Antibiotics were omitted from cultures for determination of growth rate, PG structure, cell length, and cell diameter.

Cloning of *ponA*

Each of the S, N, P and C domain-coding sequences of *ponA* was amplified by PCR using forward and reverse primers to introduce restriction sites on the ends of each domain without changing the amino acid coding capacity (Table 3a). Wild type *B. subtilis* PS832 chromosomal DNA was used as the template. The PCR products were ligated to the pGEM-T vector (Promega), transformed into *E. coli* JM109, and sequenced to verify that there were no mutations in the coding sequences. Restriction sites introduced at the ends of domains facilitated the fusion of the four domains and the reconstruction of full-length *ponA* in pGEM-T. A *Pac*I site was at the 5' end of the S domain-coding sequence where it was ligated to the pGEMT vector. A *Cla*I site at the carboxyl terminus of the S domain and at the amino terminus of the N domain fused the S and N domains (Figure 5). An *Xba*I site linked the N and P domain-coding sequences. A *Kpn*I site linked the P and C domain-coding sequences. A *Bam*HI site was at the 3' terminus of the C domain-coding sequence where it was ligated with the vector pGEMT. Plasmid pSWEET (Bhavsar, Zhao et al. 2001) was modified by A. Talu. The *bga*B gene was replaced with a linker that contains the *ponA* ribosome binding site (RBS), a new *Pac*I site and a new *Not*I

Table 2a. *B. subtilis* strains constructed

Strains	genotype	Transformation	
		Donor	**Recipient**
DPVB319	Δ*ponA*::Sp, *amyE*::1SNPC-FLAG	pDPV219	PS2062
DPVB378	Δ*ponA*::Sp, *amyE*::1SNP-FLAG	pDPV266	PS2062
DPVB379	Δ*ponA*::Sp, *amyE*::1SN-FLAG	pDPV269	PS2062
DPVB380	Δ*ponA*::Sp, *amyE*::FLAG-1SNPC	pDPV270	PS2062
DPVB381	Δ*ponA*::Sp, *amyE*::4S1NPC-FLAG	pDPV267	PS2062
DPVB401	Δ*ponA*::Sp, *amyE*::ΔS1NPC-FLAG	pDPV273	PS2062
DPVB418	Δ*ponA*::Sp, amyE::blank pSWEET	pSWEET	PS2062
[1]DPVB445	Δ*ponA*::Sp, *amyE*::1SNP*C-FLAG	pDPV215	PS2062
[2]DPVB447	Δ*ponA*::Sp, *amyE*::1SN*PC-FLAG	pDPV214	PS2062

1. A point mutation in the P domain
2. A point mutation in the N domain

Table 2b. *E. coli* strains and plasmids constructed

Strains	transformed plasmid	Plasmid genotype
DPVE77	pDPV155	*ponA* P domain in pGEMT
DPVE78	pDPV156	*ponA* C domain in pGEMT
*DPVE79	pDPV157	*ponA* S domain in pGEMT
*DPVE80	pDPV158	*ponA* N domain in pGEMT
*DPVE100	pDPV175	*ponA* SN fusion in pGEMT
DPVE89	pDPV171	*ponA* PC fusion in pGEMT
*DPVE118	pDPV185	*ponA* SNPC fusion in pGEMT
DPVE144	pDPV217	pGEM-T-1C-FLAG
DPVE147	pDPV219	pSWEET-*ponA*-FLAG

Note: Strains marked with * are constructed by Ayse Talu

Table 3a. Primers for amplification and sequencing of *ponA* sequences.

Primer name	sequence	Restriction site intr'd
1Sup	GTTAATTAAATGTCAGATCAATTTAACAGT	PacI
∆ S up	GTTAATTAAATGTCATTGTTTAAAAAGACCCTTTTCAC	
1Sdowm	ATCGATGGACGGCGCATCAGAAACC	ClaI
1Nup	ATCGATGAAAGCAAATTGAAGACG	ClaI
1Ndown	TCTAGAGTCGTATAGATCTTTAATCC	XbaI
1Pup	CAATTGGTCTAGATACAAAAGCACAAGATAAAC	XbaI
1Pdown	TTAGGTACCTGTCTTCACAGCTGTTTTCAG	KpnI
1Cup	GGTACCGGACAGCTTGCACAAG	KpnI
1Cdown	GGATCCTTTAATTTGTTTTTTCAATGGA	BamHI
4Sup	GTTAATTAAGTGACCATGTTACGAAAAATA	PacI
4Sdown	ATCGATATTTTTATCAAGCACCTGATC	ClaI
ponA-FLAG	TTA CTT GTC ATC GTC GTC CTT GTA GTC ATT TGT TTT TTC AAT GG	
ponA-P-FLAG	TTA CTT GTC ATC GTC GTC CTT GTA GTC GGT ACC TGT CTT CAC AGC TG	
ponA-N-FLAG	TTA CTT GTC ATC GTC GTC CTT GTA GTC ATC TAG AGT CGT ATA GAT C	
amyE up	AATGAGGTTAAGAGTATTCC	
FLAGrev	TTA CTT GTC ATC GTC GTC CTT GTA GTC	

Underlined is FLAG sequence.

Table 3b. Primers for introduction of point mutations in the N and P domain-coding sequences in *ponA*.

1NB	CGAGCGTCTTGTGTTGCGATAAAGGC
1NC	GCCTTTATCGCAACACAAGACGCTCG
1PB	CGGTTTTATGGTGCACCCAGGCTGTGCCTTAG
1PC	CTAAGGCACAGCCTGGGTGCACCATAAAACCG

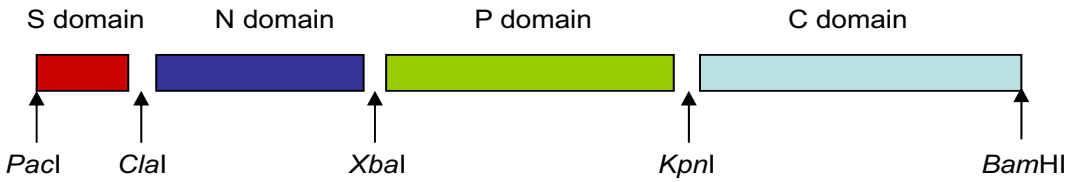

Figure 5. Reconstruction of full length PBP1. Restriction sites were introduced in PCR at the ends of each domain-coding sequence of PBP1. Domains were fused at these restriction sites, and full length PBP1 was reconstructed. The intact domains were replaced by the mutant ones to make mutated forms of PBP1.

site which allowed the insertion of the reconstructed *ponA* gene into the modified vector. In addition to the *ponA* sequence between *Pac*I and *Bam*HI, the 20 bp *Bam*HI-*Not*I sequence was from the pGEMT vector. A *Kpn*I site and one *Xba*I site in the pSWEET vector were eliminated by removing a 400 bp non-coding region. This modified pSWEET-*ponA* plasmid was denoted pDPV192. A second *XbaI* site in pSWEET close to the end of the coding sequence of *xyl*R gene, was eliminated, and an unconserved amino acid in the coding sequence of *xyl*R was mutated from aspartate to alanine. Thus the pSWEET vector was fully modified, and with the *ponA* gene inserted at *Pac*I-*Not*I sites, a pSWEET-*ponA* plasmid was constructed as pDPV196.

Cloning of C-terminal FLAG-tagged *ponA*, and FLAG-tagged *ponA* mutants

The coding sequences for PBP1C-FLAG (carboxyl terminal FLAG-tagged PBP1 C domain), PBP1P-FLAG, and PBP1N-FLAG were amplified using reverse primers ponA-FLAG, ponA-P-FLAG, and ponA-N-FLAG (Table 3a), and the corresponding forward primers, and were ligated to the pGEMT vector. Truncated PBP1S and PBP4S domain-coding sequences were amplified and ligated to pGEMT. Mutagenic primers were used in PCR to introduce single point mutations in the active site of the N and P domain-coding sequences of *ponA* (Table 3b) (Ho, Hunt et al. 1989). They were then used to replace the intact domains of *ponA* in pSWEET-*ponA* (pDPV196), and to add a carboxyl FLAG tag, using restriction sites present at the ends of the domains or *NotI* as the downstream cloning site linking to pSWEET, to form plasmids pSWEET-ponA-FLAG, pSWEET-PBP1SNP-FLAG, pSWEET-PBP1SN-FLAG, pSWEET-Δ1SNPC-FLAG, pSWEET-4S1NPC-FLAG, pSWEET-1SN*PC-FLAG and pSWEET-1SNP*C-FLAG. The presence of carboxyl terminal FLAG of mutant *ponA* in the pSWEET vector was verified by DNA sequencing using the amyEup primer (Table 3a).

Growth rate, cell length and PG structure analysis

Cell phenotypic analysis for the *B. subtilis* strains included the growth rate, cell length, cell diameter and PG structure. The *B. subtilis* strains were inoculated in 100 ml

2xSG medium with or without supplementation of 0.4% xylose and were incubated at 37° C with aeration. Growth rate was measured as doubling time and the optical density was read at 600 nm (OD600) using a spectrophotometer (Genesys 5). For PG sample preparation, at OD600=1.0, 50 ml of the culture was cooled down quickly by swirling in an ice/water bath for 5 min. Cells were harvested by centrifugation at 15 k g at 4° C for 10 min, and resuspended in 2 ml cold dH_2O. The cold cell suspension was dripped into 50 ml of boiling and stirring 4% SDS to be boiled for 30 min. After cooling to room temperature, PG was pelleted at 12 k g at room temperature for 6 min. It was washed in 20 ml of dH_2O four times to remove SDS and was frozen at -80° C. PG was further purified, muramidase digested, and analyzed using HPLC as previously described (McPherson and Popham 2003). At OD600 0.5, for cell length and diameter measurement, cells from 1 ml of culture was collected by centrifugation at 2.5 k g for 1 min at room temperature, and fixed in 1 ml 3.3% glutaraldehyde for 1 hour at room temperature. Cells were pelleted and resuspended in dH_2O and preserved in 0.2% sodium azide at 4° C. Fixed cells were applied to poly-lysine coated microscope slides and visualized with a phase-contrast Olympus IX 81 microscope using Slidebook 4.1 software (Olympus). For each strain, the length and width of about 300 randomly selected cells were measured.

PBP1-FLAG expression, protein extraction and western blotting

PBP1-FLAG protein was expressed in *B. subtilis* with induction using 0.4% xylose to achieve PBP1 expression level similar to that of wild type *B. subtilis* cells. To extract total cell proteins, *B. subtilis* cells were harvested from 20 ml log phase culture (OD600=0.5) incubated at 37 ° C with aeration and addition of 0.4% xylose. Cells were washed with 1 ml cold PBS (137 mM NaCl, 2.7 mM KCl, 4.3 mM $NaHPO_4$, 1.4 mM KH_2PO_4, pH 7.3) supplemented with 1 mM beta-mercaptoethanol and 0.1 mM phenylmethylsulphonylfluoride. Then cells were broken in the same buffer by sonication on ice in 10 second bursts with 10 seconds pause between each burst for 4 min. Cell debris was removed by centrifugation at 10 k g for 5 min at 4ºC and the supernatant was used for

western blotting. Blots were probed using 2 μg/ml anti-FLAG M2 Abs (Stratagene) and 1: 5000 diluted goat anti-mouse peroxidase-conjugated IgG (Roche), and visualized using chromogenic POD substrate (Roche).

Immunofluorescence procedure: fixation, permeabilization, staining, microscopy and photography

The preparation of microscopy samples was essentially the same as previously published (Harry, Pogliano et al. 1995; Pedersen, Angert et al. 1999). *B. subtilis* cultures were incubated in 2xSG at 37 ºC with aeration until the OD600 reached 0.7. Cells from 0.5 ml of culture were harvested in microcentrifuge tubes at 2.5 k g for 1 min and fixed in 1 ml fixation buffer containing 4.4% (wt/vol) paraformaldehyde and 28 mM $NaPO_4$ pH 7.2 at room temperature for at least 20 min. After washing three times with PBS buffer, cells were resuspended in 100 μl GTE buffer (50 mM glucose, 20 mM Tris-HCl pH 7.5, 10 mM EDTA) and digested with 0.2 mg/ml lysozyme at room temperature for 6 min. Cells were then washed twice with PBS to remove lysozyme, resuspended in 100 μl PBS, and applied to poly-lysine coated multi-well microscope slides. After 30 min. to allow cells to attach to the slides, extra liquid was drained, and slides were washed twice and allowed to dry briefly. Slides were blocked with 2% (wt/vol) BSA in PBS for 20 min. at 30^{o} C and probed with 2.5 μg/ml anti-FLAG antibody (Stratagene) in PBS and 0.1% BSA for 1 hour at 30^{o} C. Slides were then washed six times with PBS and incubated with 1:400 diluted biotinylated goat anti-mouse IgG (Invitrogen) in PBS and 0.1% BSA for 1 hour at 30^{o} C. After washing six times, slides were incubated with 1 μg/ml Cy3-streptavidin (Jackson ImmunoResearch Lab), 0.2 μg/ml of fluorescein isothiocyanate (FITC)-conjugated wheat germ agglutinin (WGA) (Invitrogen), and 1 μg/ml of DAPI stain, for 1 hour at 30^{o} C. Slides were washed six times with PBS, and then were mounted with Golden anti-fade reagent (Invitrogen). Fluorescence signal was detected using an Olympus IX 81 microscope and Slidebook 4.1 software, with exposure time 500 ms for DAPI, 100 ms for FITC, and 200 ms for Cy3.

RESULTS

Construction of PBP1 mutant strains. To study the localization and the phenotypic effects of mutant forms of PBP1, eight *B. subtilis* strains were constructed (Table 2a) (Figure 6). All mutated *ponA* genes were cloned with a C-terminal FLAG tag in a modified pSWEET vector (Bhavsar, Zhao et al. 2001) (Figure 7), and were integrated into the PS2062 (*ponA* deletion null mutant) (Popham and Setlow 1995) chromosome at the *amyE* locus via a double-crossover.

DPVB319 expressed full length PBP1 without mutation. This strain has a phenotype similar to the wild type strain PS832 and was used as the positive control to study the phenotypes of other PBP1 mutants. DPVB418 has an empty pSWEET vector sequence inserted in the genome of the PBP1 null mutant. The phenotype of this strain is similar to the PBP1 null mutant PS2062 and served as the negative control in phenotypic studies of the six other PBP1 mutant strains. In DPVB378 the C domain-coding sequence of *ponA* (after 1677 bp of *ponA*) was removed and a FLAG tag was fused to the carboxyl terminus of the P domain (Figure 6). PBP1 was expressed with the lack of the C-terminal 355 amino acids. In DPVB379 the P and C domain-coding sequences of *ponA* (after 981 bp) were removed, and the FLAG tag was added to the C-terminus of the N domain. In DPVB381 the S domain of PBP1 was replaced by the PBP4 S domain. In DPVB401, the cytoplasmic region of the PBP1 S domain was deleted (before 96 bp of *ponA*), removing the first 32 amino acids of PBP1. A point mutation in Ser390 in the first conserved region in the P domain was previously shown to lead to a loss of transpeptidase activity in several other PBPs (Takasuga, Adachi et al. 1988; van der Linden, de Haan et al. 1994). A corresponding point mutation was constructed in *B. subtilis ponA* to convert Ser390 to Cys in DPVB445. A point mutation in Glu115 in the first conserved region in the N domain of *E. coli* PBP1b abolished almost completely the transglycosylase activity (Terrak, Ghosh et al. 1999). A corresponding point mutation was constructed to convert Glu115 to Gln in

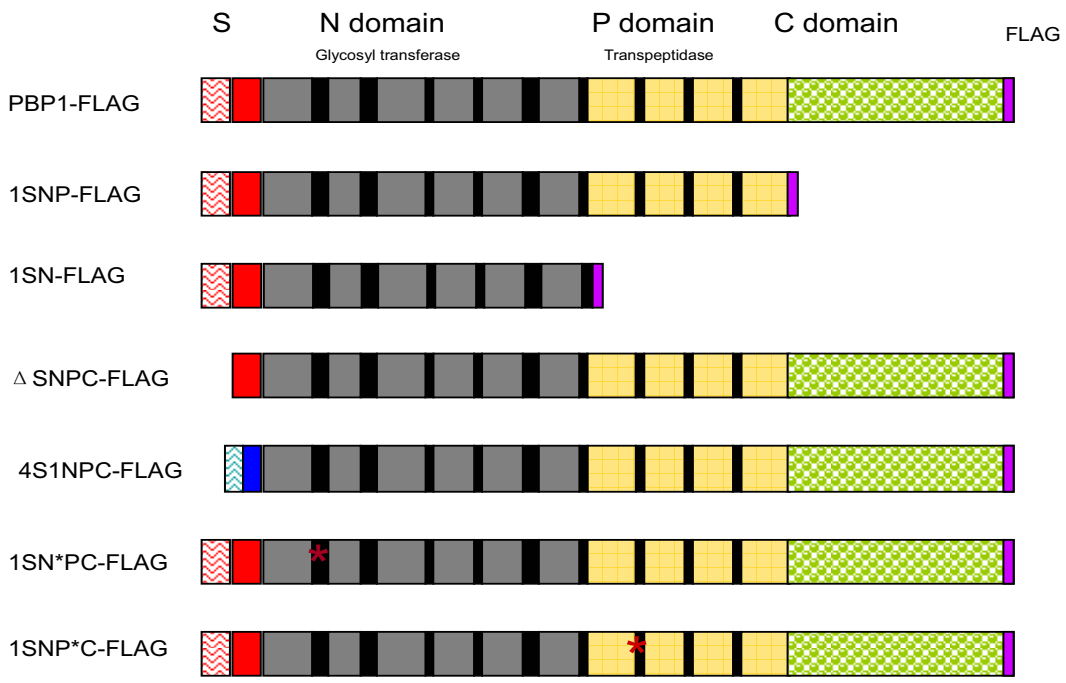

Figure 6. PBP1 composition and mutants constructed. There are four domains in PBP1: S (red), N (gray), P (yellow) and C (green) domains. The S (signal) domain is composed of a cytoplasmic tail (wavy block) and a membrane-spanning region (red block). PBP4 S domain is depicted in blue. Black blocks represent the conserved sequences in the N and P domains. Stars stand for the point mutations in the active site of the N and P domains. Purple boxes represent the FLAG peptide epitopes at the carboxyl terminus.

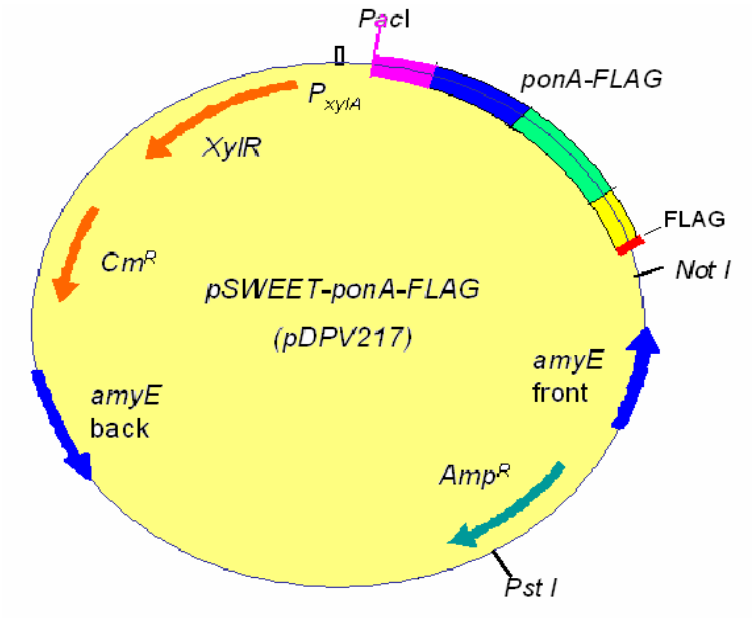

Figure 7. Map of plasmid *pDPV217* (*pSWEET-ponA-FLAG*). The pSWEET vector (A. P. Bhavsar, et al, 2000) was modified. The modified vector contains a xylose promoter (P_{xylA}), which facilitates controlled protein expression by induction with xylose at different concentrations. The *amyE front* and *back* sequences allow integratation of the linearized plasmid (by *Pst*I) into the *B. subtilis* chromosome via a double crossover at the *amyE* site. The plasmid also has an ampicillin resistance cassette (Amp^R) and a replication origin (*ori*), for routine cloning steps in *E. coli*. The chloramphenicol cassette (Cm^R) allows selection of *B. subtilis* transformants using chloramphenicol. The *ponA-FLAG* sequence was cloned in the *Pac*I/*Not*I sites. FLAG was at the C-terminus of *ponA*.

B. subtilis ponA in DPVB447. This point mutation abolished the transpeptidase acitivity of PBP1 (data not shown).

Colony Morphology of PBP1 mutants. *B. subtilis* mutant strains were streaked on rich medium 2xSG with or without addition of 0.4% xylose. Without induction with xylose, colonies of all eight strains exhibited smooth and raised edges, with flat centers (Figure 8). This is the typical phenotype of a PBP1 null mutant reported previously (Popham and Setlow 1995). With addition of xylose to the medium, colonies of the positive control and strains expressing PBP1 without the cytoplasmic region of the S domain, or with PBP4 S domain, showed raised centers and irregular edges, which was the typical phenotype of wild type *B. subtilis* colonies (Popham and Setlow 1995). The colonies of the strain having a point mutation in the P domain had raised and slightly-wrinkled centers as the wild type, but they grew much more slowly. Strains cloned with PBP1 lacking the C domain, without both P and C domains, with a point mutation in the N domain, and the negative control had colonies similar to a PBP1 null mutant even in the presence of 0.4% xylose.

Growth of PBP1 mutants. The growth rates of all eight strains were measured and expressed as doubling times in rich medium 2xSG with 0.4% xylose (Table 4). The OD600 of each culture was recorded until it exceeded 4.0 (Figure 9). The growth rate of the positive control was the highest and the doubling time was 23 min. The doubling time of the negative control was 27 min. Removal of the cytoplasmic region of the PBP1 S domain did not change the doubling time. All other mutations resulted in slower growth rates. Growth after log phase was studied as the time each strain took to grow from OD600 1.0 to 3.0. The positive control grew faster than any other strain and it took 68 min to grow from OD600 1.0 to 3.0. The negative control took 111 min. The time taken by strains cloned with PBP1 with altered S domains, without C domain, or without both P

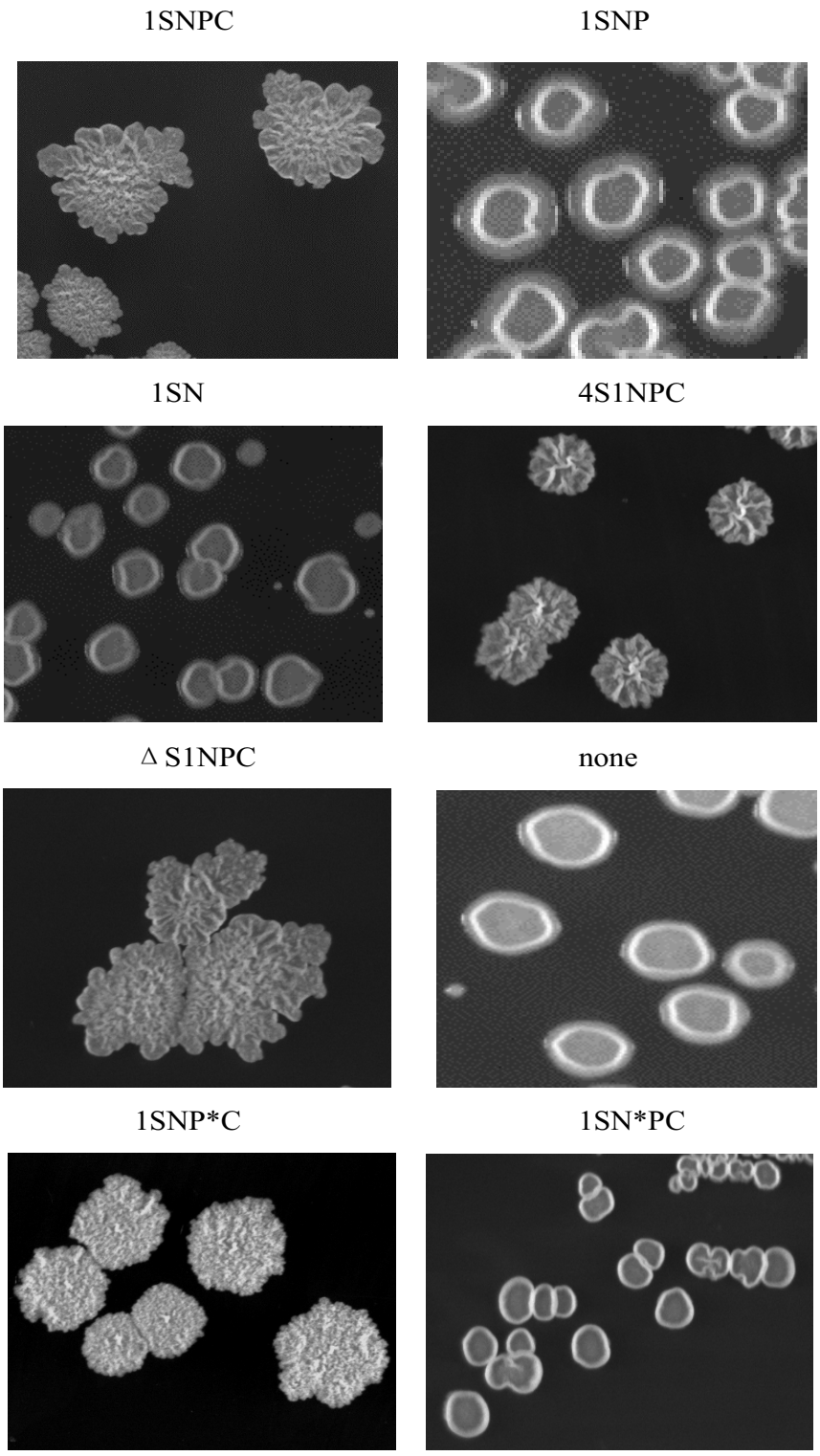

Figure 8. Colony morphology of PBP1 mutants. All strains were grown on rich medium 2xSG supplemented with 0.4% xylose at 37 ºC.

Table 4. Growth of PBP1 mutants[a].

Strain	Protein expressed	Doubling time[b] (min)	Time for growth[c] from OD600 1.0 to 3.0 (min)
DPVB319	1SNPC-F	23	68
DPVB378	1SNP-F	27	91
DPVB379	1SN-F	26	94
DPVB381	4S1NPC-F	26	87
DPVB401	Δ S1NPC-F	23	70
DPVB418	No PBP1	27	111
DPVB445	1SNP*C-F[d]	27	162
DPVB447	1SN*PC-F[d]	28	181

a. Growth was in 2xSG at 37° C.

b. Doubling times were averages from at least three separate experiments.

c. Growth to above OD600 3.0 was averaged from at least two separate experiments.

d. Star* stands for the point mutations made at the active sites in the P or N domains.

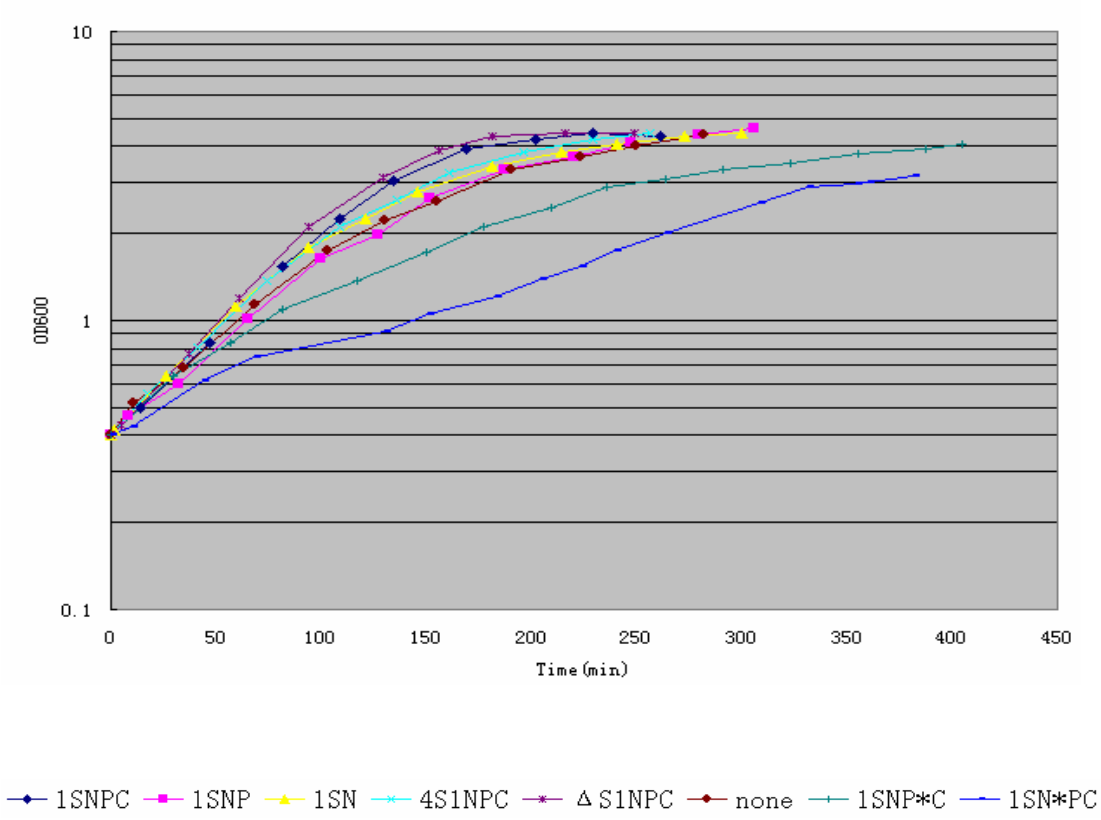

Figure 9. Growth of PBP1 mutant strains. All strains were grown in rich medium 2xSG supplemented with 0.4% xylose and antibiotics chloramphenicol (3 µg/ml), spectinomycin (100 µg/ml) at 37° C with aeration. OD600 was measured every 20 to 30 min until above 4.0. Growth above OD600 4.0 of the strain expressing PBP1 with a point mutation in the N domain was not shown.

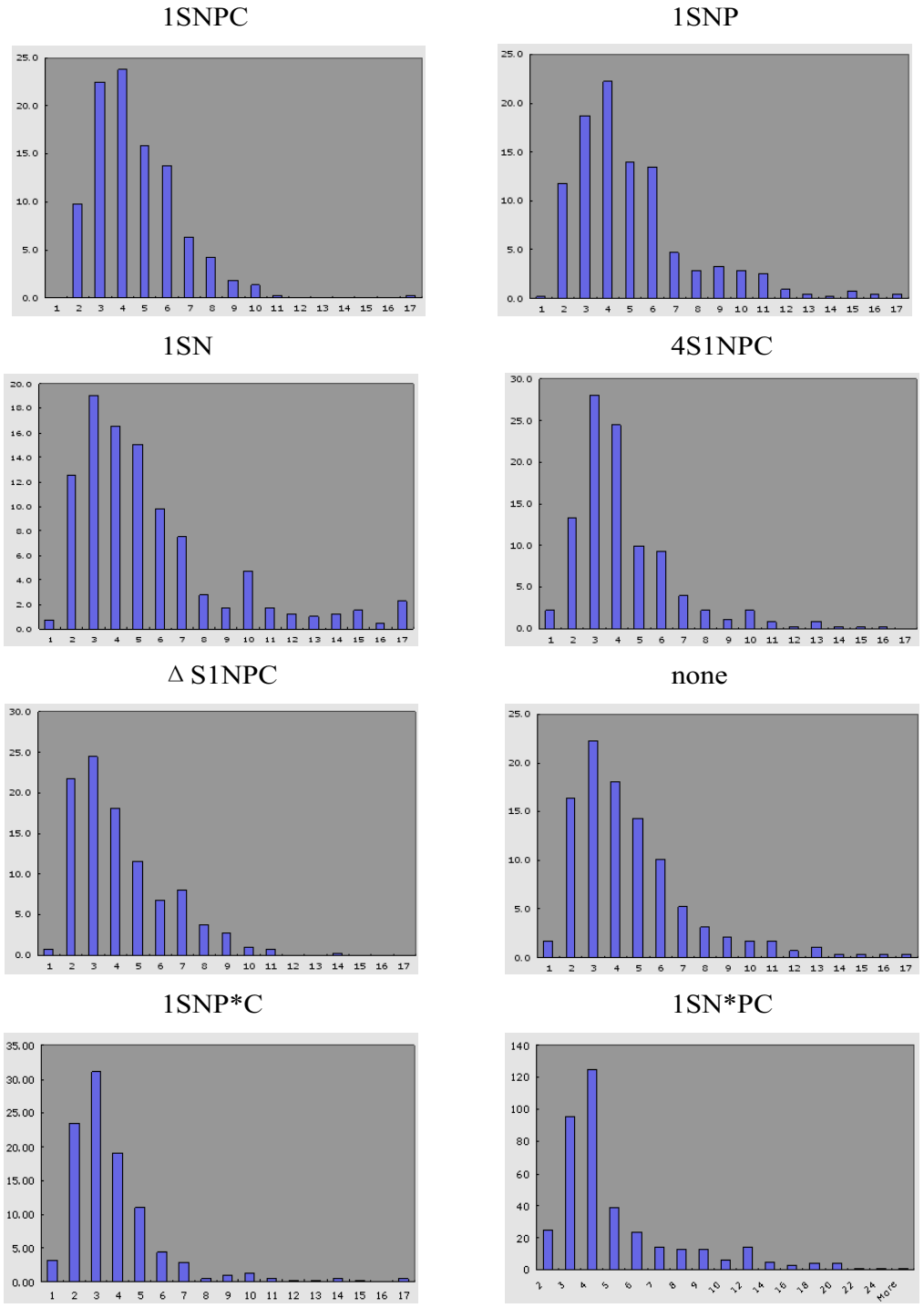

Figure 10. Cell length distribution of PBP1 mutants. All strains were grown in rich medium 2xSG supplemented with 0.4% xylose at 37° C with aeration. About 300 log-phase cells were measured and analyzed. The x-axis is bin, and the y-axis is percent of cells that fall into each bin of cell length (μm).

and C domains, was in between these two times. Surprisingly, mutant strains with single point mutations in the active site of either N or P domain grew apparently more slowly than the negative control, and they took 162 min and 181 min, respectively.

Cell morphology of PBP1 mutants. The cell length and diameter (Figures 10 and 11) were measured on log-phase cells using a phase-contrast microscope and the Slidebook 4.1 software. In agreement with previous reports, the negative control had more long and slightly-bent cells than the positive control though the average cell length was similar (Table 5). The percentage of cells longer than 10 μm in the cell population increased from 1.93% in the presence of PBP1 in the positive control to 8.14% in the absence of PBP1 in the negative control (Table 5). The percentage of long cells in strains expressing PBP1 without the C domain or with altered S domains fell in between these two numbers. The other strains with PBP1 lacking both P and C domains, or with point mutations had a higher percentage of cells longer than 10 μm, which was comparable to the negative control. Cell diameters were averaged from more than 50 cells for each strain. It varied from 0.9 μm in the negative control to 1.2 μm in the positive control (Table 5). Removal of the cytoplasmic region of the S domain did not affect the diameter. While other mutations all resulted in the decreased cell width (Table 5)..

Structural analysis of vegetative PG from PBP1 mutant strains. Muropeptides were extracted from log phase cells, purified and separated using reversed phase-high pressure liquid chromatography. In the positive control the PG crosslinking percentage was 28.2%. The crosslinking decreased to 23.9% in the same strain when no xylose inducer was added to the growth medium, and to 23.7% in the negative control. The strain cloned with PBP1 lacking both P and C domains had a similar low crosslinking rate 23.8% as the negative control. The crosslinking of other strains were intermediate between the two rates.

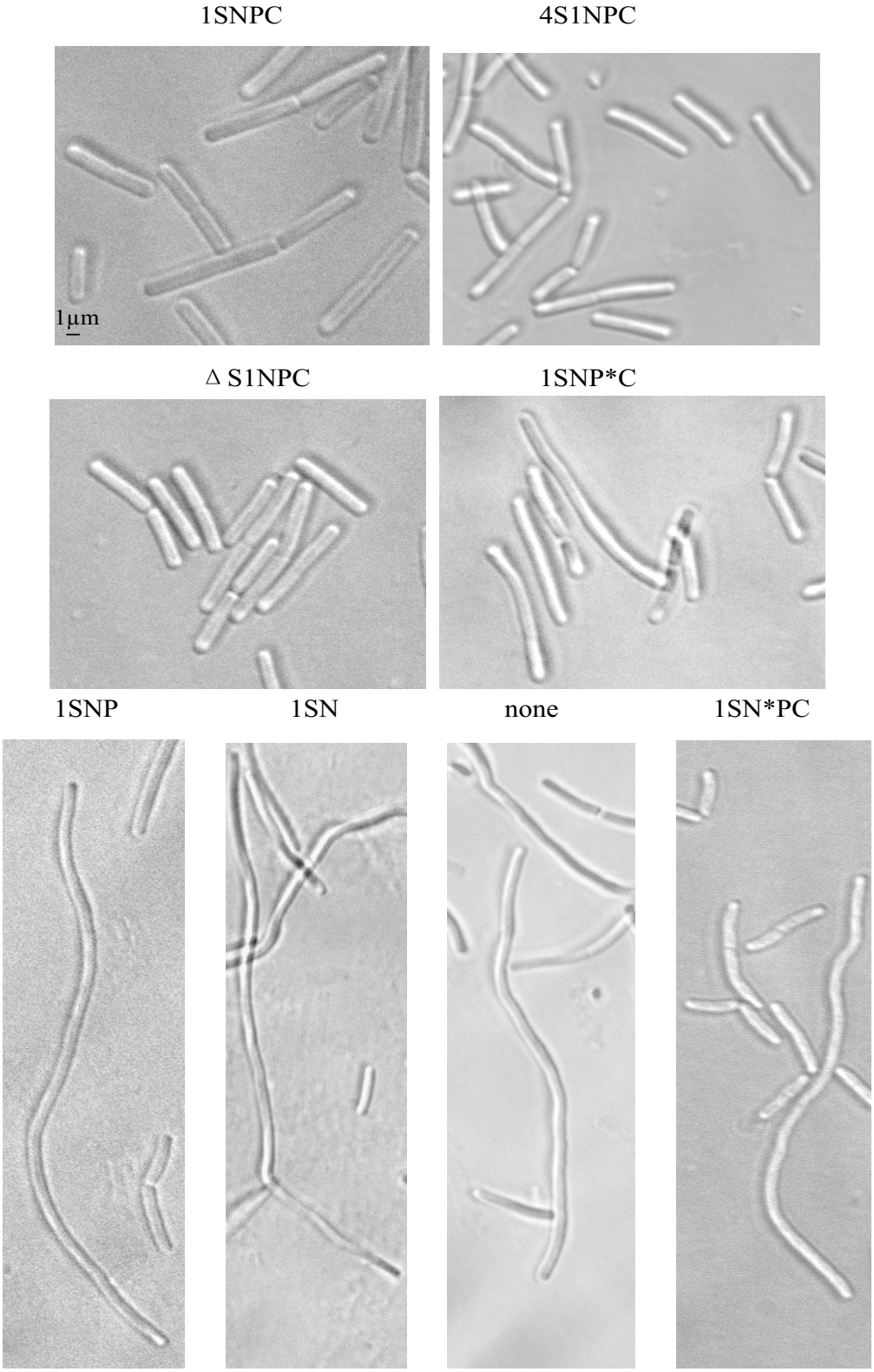

Figure 11. Cell morphology of PBP1 mutant strains. Bar in the up left panel denotes 1 μm. All pictures are in the same magnification.

Table 5. Average cell length and diameter in PBP1 mutant strains.

Strain	Cell Length			Cell Width	
	Average Cell Length (µm)	% Cells >10 µm	Number of Cells Measured	Cell Width (µm)	Number of Cells Measured
1SNPC	5.18	1.93	378	1.19	55
1SNP	5.93	7.99	423	0.91	62
1SN	6.64	12.00	399	0.90	59
4S1NPC	4.98	5.49	352	0.96	52
Δ S1NPC	4.76	3.01	397	1.20	55
No PBP1	5.45	8.14	287	0.92	53
1SNP*C	4.45	3.42	409	0.95	65
1SN*PC	4.82	8.52	387	0.94	62

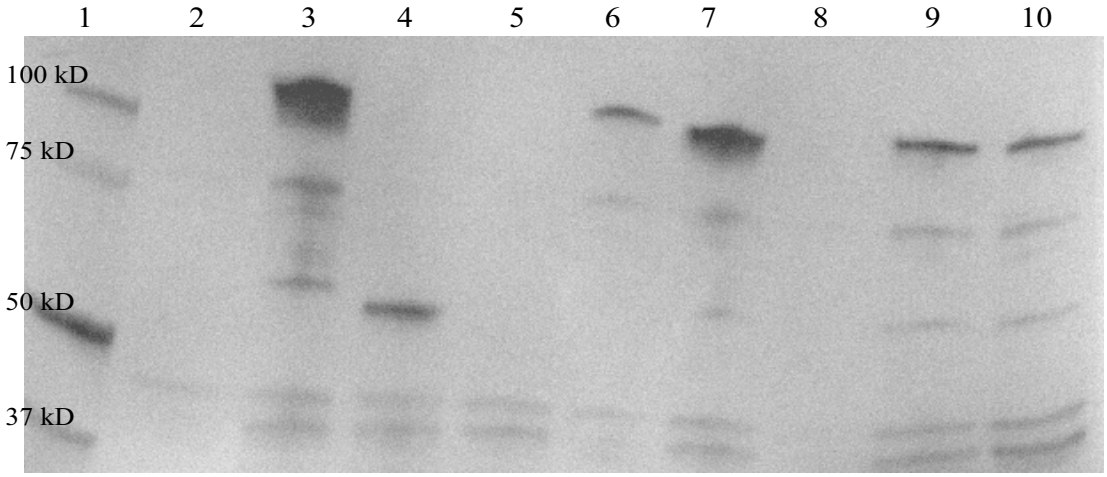

Figure 12. Immunoblot analysis of the expression of PBP1 variants in log phase cultures. All strains were grown in rich medium 2xSG supplemented with 0.4% xylose otherwise indicated, at 37° C with aeration. Proteins were extracted from log phase cultures, and separated by 10% SDS-PAGE. Detection of FLAG-tagged PBP1 proteins used anti-FLAG antibodies. Cells were expressing: no PBP1 (lane 2, DPVB319 with no xylose included in the growth medium), PBP1 (lane 3, positive control, DPVB319, MW 110 kD), 1SNP (lane 4, DPVB378, MW 62 kD), no 1SN (lane 5, DPVB379, calculated MW 37 kD), 4S,1NPC (lane 6, DPVB381, MW 110 kD), ∆S,1NPC (lane 7, DPVB401, MW 110 kD), no PBP1 (lane 8, negative control, DPVB418), 1SNP*C (lane 9, DPVB445, MW 110 kD), 1SN*PC (lane 10, DPVB447, MW 110 kD).

Expression of PBP1 variants. All PBP1 variants were C-terminal tagged by the small FLAG peptide. The expression of PBP1 proteins with induction of xylose was examined by western blotting using anti-FLAG antibodies. 10 μg of total proteins from each of the eight strains, and one extracted from the positive control strain without addition of xylose in the growth medium, were loaded in each lane of a SDS-PAGE gel. Except in the negative control and in the strain cloned with PBP1 lacking both P and C domains, all other strains had FLAG-tagged proteins expressed (Figure 12). A 62 kD band was detected in accordance to the calculated size of PBP1SNP-FLAG in lane 4. PBP1 with altered S domains (lanes 6 and 7), with point mutations (lanes 9 and 10), and in the positive control (lane 3) were expressed and showed at positions around 110 kD, which agreed with their calculated molecular weight.

Localization of mutant PBP1. Localization of FLAG-tagged PBP1 variants, cell walls and DNA of the *B. subtilis* cells were stained using Cy3, FITC, and DAPI, respectively. In 97% of the positive control cells, PBP1-FLAG localized to the septum (Figure 13, B, indicated by arrows) (Table 6). This localization specificity agreed with previous studies (Pedersen, L., et al. 1999). In the negative control and the strain cloned with PBP1 lacking both P and C domains, little or no Cy3 signal was detected (Figure 13, T and W) (Table 6). This is consistent with the lack of detectable PBP1 proteins in these strains (Figure 12). PBP1 lacking the C domain, with a PBP4 S domain, or with a point mutation in the N domain, has no specific localization (Figure 13, E, H, K) (Table 6). PBP1 with a truncated S domain, and PBP1 with a point mutation in the P domain, had decreased localization specificity and only some signal was detected to localize at the septum (Figure 13, N, Q, indicated by arrows). It should be noted that in these strains some Cy3 signal was detected adjacent to the septum (Figure 13, E, H, K, indicated by blunt arrows), and this was not considered as septum-localization in this study.

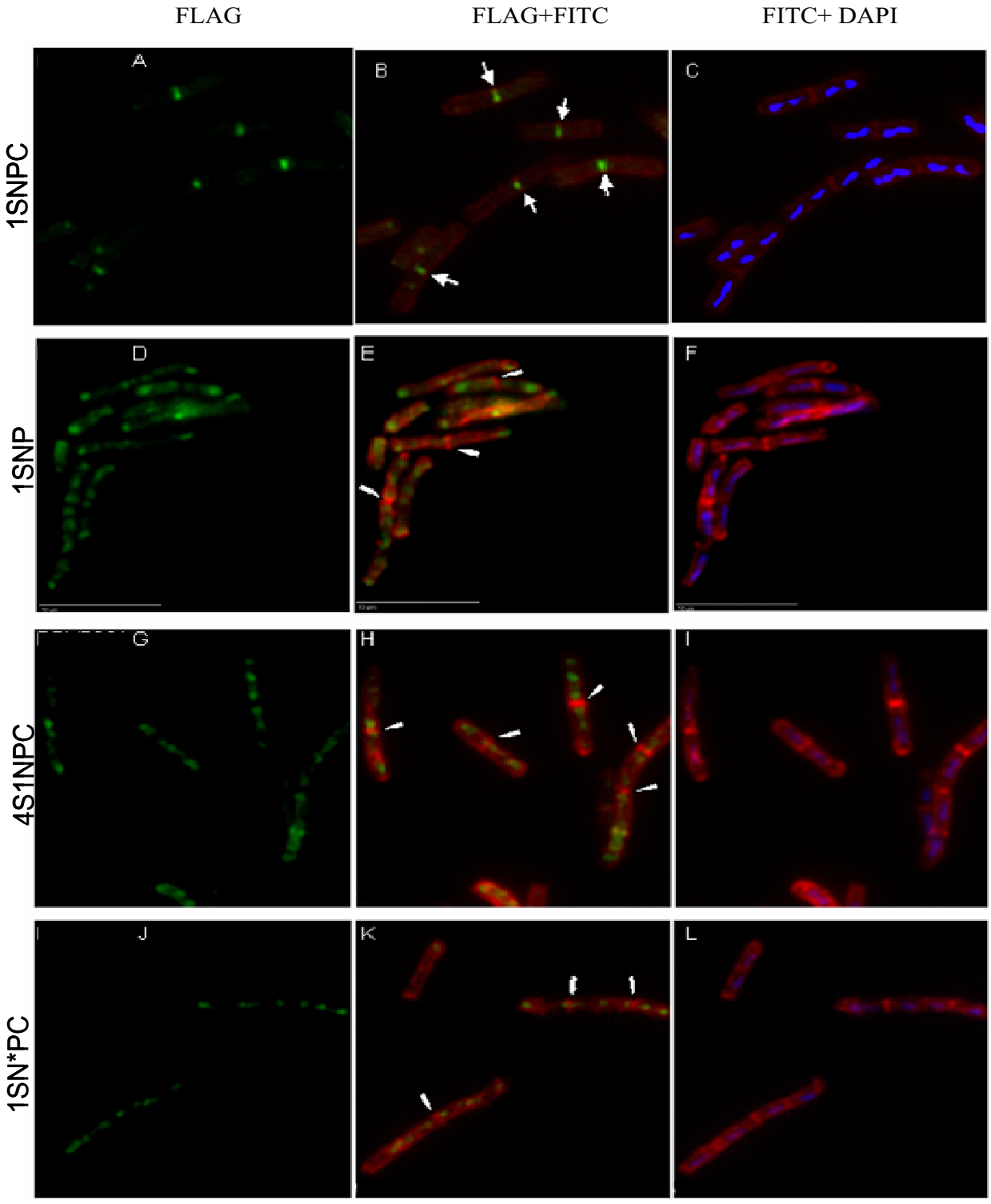

Figure 13. Fluorescence micrographs of cells expressing mutant PBP1. Bar in panel D denotes 10 μm and all pictures are in the same magnification. Arrows in panel B point to the septum-localized PBP1. Blunt-end arrows in panels E, H and K indicate that some altered PBP1 proteins localize adjacent to but not on the septum.

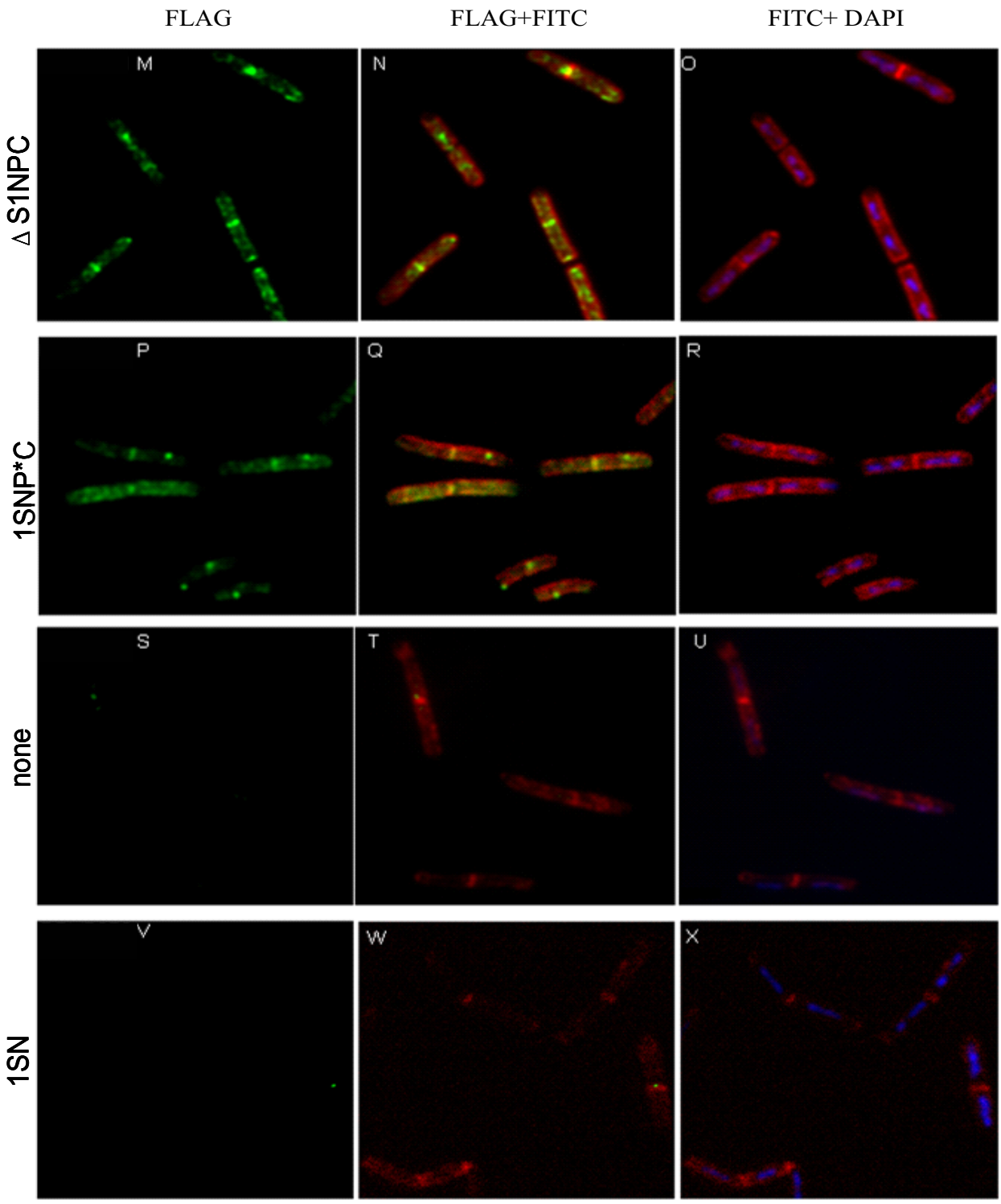

Figure 13 continued. PBP1 without the cytoplasmic region of the S domain (panel N), and PBP1 with a point mutation in the active site of the P domain (panel Q), has a decreased septum-localization specificity.

Table 6. PBP1 localization analysis in PBP1 mutants.

PBP1[b] protein	Localization in cells with septum[a]					Localization in cells without septum[a]			
	Number of cells counted	Septum	Poles	Other places	None	Number of cells counted	Poles	Other places	None
1SNPC-F	76	97%	4%	32%	3%	12	25%	25%	50%
1SNP-F[c]	20	33%	15%	60% [c]	40%	30	0	17%	83%
1SN-F	38	0	0	5%	95%	38	0	3%	97%
4S1NPC-F[c]	38	26%	3%	66% [c]	21%	76	0	76%	24%
Δ SNPC-F	38	87%	0	97%	3%	59	0	100%	0
No PBP1	35	0	3%	20%	77%	38	0	24%	76%
1SNP*C-F	55	100%	7%	64%	4%	53	0	100%	0
1SN*PC-F[c]	38	24%	3%	63% [c]	34%	36	0	72%	28%

a. Growth was in 2xSG at 37° C.

b. Cy3-PBP1-FLAG in all strains was exposed for 200 ms. The signal was cut off at 800 ms, and the localization was studied in more than 50 cells for each strain.

c. Some fluorescence signal of PBP1 with PBP4 S domain, without C domain, or with a point mutation in the N domain, was detected adjacent to but not on the septum.

DISCUSSION

Previous studies of class A PBPs have demonstrated that the glycosyl transferase is contained within the N domain, and the transpeptidase is contained within the P domain. The C domain has no apparent enzymatic activity but its loss can alter the cell phenotype. In wild type *B. subtilis*, PBP1 localizes specifically to the septum and is part of the division apparatus. A *B. subtilis* PBP1 null mutant has slightly reduced growth rate, cell diameter, and PG crosslinking, and has dramatically decreased sporulation efficiency. In the cell population there are more relatively long cells. We here report the construction and phenotypic examination of six strains with altered forms of PBP1: two with domain deletions (without the C domain; with no P and C domains), two with S domain mutations (with the S domain replaced by the PBP4 S domain; with the removal of the cytoplasmic region of the S domain), and two with point mutations in the enzymatic active site (in the P domain; in the N domain). With induction using 0.4% xylose, the colony and cell morphologies of the positive control strain that expressed full length PBP1 without mutations were similar to the wild type, and PBP1 localized specifically to the septum. The negative control had no PBP1 expressed at the presence of xylose, and its phenotype was similar to the PBP1 null mutant.

The mutant expressing PBP1 without the C domain exhibited phenotypic traits intermediate between the wild type and the PBP1 null mutant. The protein lost its septum-localization specificity. All these suggest that even though the C-terminal region has no defined enzymatic activity, it aids in the maintenance of a functional PBP1. The C domain may be involved in the interaction of PBP1 with other proteins or with PG components. PBP1 lacking both P and C domains was very unstable and this mutant had phenotypic traits comparable to the null mutant.

When the PBP1 S domain was lacking its cytoplasmic tail or was replaced by the PBP4 S domain, the PBP1 variants could still be stably expressed and the phenotypic

changes were minor in comparison with the wild type. Furthermore, quantitative measurement in doubling time, cell diameter, percentage of long cells in the cell population, PG crosslinking percentage, and time for growth from OD600 1.0 to 3.0, showed that PBP1 lacking its cytoplasmic tail is functionally more close to the wild type than the protein with the PBP4 S domain. These results reveal that the cytoplasmic region of the S domain has a minor effect on the PBP functions and cell phenotypes. Localization studies showed that the PBP4 S domain abolished the protein's localization specificity, while the loss of the cytoplasmic region did not have much of an affect on the protein localization. Combined with the knowledge that PBP4 localizes to the lateral wall in the wild type vegetative *B.subtilis* (Scheffers, D.J., L.J.F. Jones, and J. Errington. 2004), it appears that the S domain of PBP1 plays an important role in localization and function.

Surprisingly, mutants with single point mutations in the active site of the N and P domains showed dramatic phenotypic changes, some of which exceeded those of the PBP1 null mutant. This difference is most obvious in the time for growth. Strains with point mutations in the P and N domains took 162 and 181 min, respectively, for growth from OD600 1.0 to 3.0, which was significantly longer than 111 min by the negative control strain with no PBP1 expressed. It is known that the mutation in the N domain disrupted its glycosyl transferase activity (data not shown), and it is expected that the mutation in the P domain removed its transpeptidase activity. PBP1 with the point mutation in the N domain dispersed all over the cell, while the point mutation in the P domain reduced slightly the protein localization specificity at the septum. All these findings suggest that the N domain is crucial for PBP1's function and cell growth, and that a functional PBP1 which is important in cellular mechanisms may be an important component of superior complexes.

Overall, a model is proposed for the structure and function of a PBP1-containing complex (Figure 14) that can well explain why point mutations in the enzymatic active sites affect cell growth more than a lack of PBP1. Within PBP1 the GT and TP activities

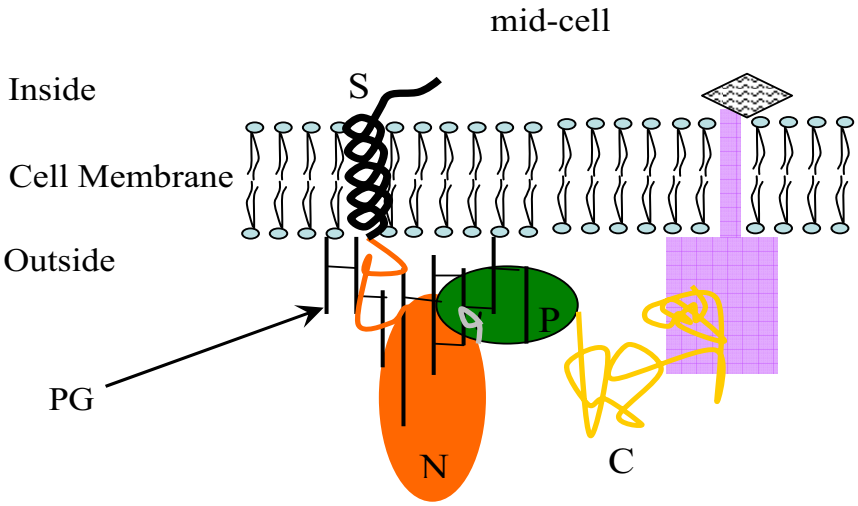

Figure 14. Model proposed in this study for the functioning of PBP1 domains. The S domain (helix and the cytoplasmic tail) acts as the initial force and membrane anchor to localize PBP1 at cell division sites. The N domain (orange oval) then binds and polymerizes the glycan strands. These bonds strengthen the septum-localization of PBP1. The P domain (green oval) cooperates with the GT activities associated with the N domain, and functions as TP to crosslink the peptide side chains of the incorporated glycan units. The C domain (yellow) is involved in the interaction with other proteins directly or indirectly (purple boxes and wavy diamond). With removal of the C domain, the protein association is disrupted, and PBP1 can no longer localize at the septum.

cooperate to function, maybe by inter-domain interactions. The glycan strands are polymerized by the glycosyl transferase carried out by the N domain, and the peptide side chains are used as substrates for the adjacent P domain to be crosslinked. The protein interaction is not inhibited by a single point mutation in either domain; however, lack of one enzymatic activity could inhibit PBP1's functions as a whole. In the absence of PBP1, other PBPs could compensate for PBP1's function. But when PBP1 is present the compensation activities could be inhibited, possibly due to the space or substrate limitation which are already occupied by or bound to PBP1.

Furthermore, the S domain may act as the initial force to localize PBP1 to the septum, and when it is replaced by the PBP4 S domain, the protein lost its localization specificity. At the septum, the N domain binds to the glycan strands, and the bonds reinforce the localization. Similarly, in *S. aureus*, binding to the PG substrates is necessary for the septum localization of class A PBP2 (Pinho and Errington 2005). The point mutation in the active site of N domain disrupted the substrate binding, and the association between the S domain and the mid-cell membrane was too weak to hold the protein at the septum, so PBP1 defused to other places in the cell. The mutation in the active site of the P domain removed its transpeptidase activity, but one amino acid probably won't have much of an affect on the protein localization.

The C domain has no obvious enzymatic activity but the lack of it affected the cell phenotypes, and delocalized PBP1. It may be involved in the interactions between PBP1 and other proteins, to form a complex. It may also aid in the protein's localization at the septum. With the removal of the C domain, the protein association with other proteins is disrupted, and PBP1 localizes nonspecifically. The C domain is necessary but not sufficient for the septum localization of PBP1, so are the S and functional N domains.

The findings of this work provide more information on the functions of PBP1 domains and certain regions, and more indirect proof of PBP1-involved cooperative protein complexes, permitting the proposal of a model describing how PBP1 functions in a

cellular environment. Additional discussion and research direction will have to involve the proteins that may be interacting with PBP1 directly or indirectly at the septum, and they may not be PG synthesis- or modification- related proteins. The candidate proteins could be other class A or B PBPs (e. g. PBP2b), lytic enzymes, cytoskeleton proteins (e.g. MreB, Mbl), or other proteins. In the Gram negative bacterium *E. coli,* based on known interactions, a divisome includes several complexes: a Z-ring complex, a Fts Q/L/B complex, and a PG synthetic complex (Goehring, Gonzalez et al. 2006). In *B. subtilis*, a model has been proposed that suggested that PBPs interact with cytoskeletonal proteins to synthesize PG and determine cell shape (Stewart 2005) (Figure 4). The findings and model proposed in this work reveal the functions of PBP1 domains and certain regions.

Several approaches may be applied on future studies on PBP1 domains and PBP1-protein interactions. One approach is construction of chimeric proteins for example 1S-4NP-1C (PBP4 with the S domain replaced by the PBP1 S domain, and the C domain replaced by the PBP1 C domain), having it transformed into the PBP1/4 double null mutant, and studying the morphologies as well as the protein localization. If the model proposed by this work is correct, it is expected that the chimeric protein preferentially localizes at the septum, and the morphologies of the mutant strain is similar to that of the PBP1 null mutant. The second approach is studying PBP1-protein interactions using fluorescence resonance energy transfer (FRET). PBP1 and the potential PBP1-interacting proteins for example MreC or PBP2b, are labeled by different fluorescein. When in vivo the donor protein PBP1 is excited, if the candidate protein is interacting with PBP1, it can absorb the emission energy and generate a detectable signal. Functional and interaction studies of the major vegetative PG-synthetic protein PBP1 in the Gram positive model bacterium *B. subtilis* can contribute to the thorough understanding of bacterial PG synthesis mechanism and antibacterial development.

REFERENCES

1. Adam, M., C. Fraipont, N. Rhazi, M. Nguyen-Disteche, B. Lakaye, J. M. Frere, B. Devreese, J. Van Beeumen, Y. van Heijenoort, J. van Heijenoort, and J. M. Ghuysen. 1997. The bimodular G57-V577 polypeptide chain of the class B penicillin-binding protein 3 of *Escherichia coli* catalyzes peptide bond formation from thiolesters and does not catalyze glycan chain polymerization from the lipid II intermediate. J Bacteriol **179**:6005-9.

2. Alaedini, A., and R. A. Day. 1999. Identification of two penicillin-binding multienzyme complexes in *Haemophilus influenzae*. Biochem Biophys Res Commun **264**:191-5.

3. Anagnostopoulos, C., and J. Spizizen. 1961. Requirements for Transformation in *Bacillus Subtilis*. J Bacteriol **81**:741-6.

4. Anderson, J. S., P. M. Meadow, M. A. Haskin, and J. L. Strominger. 1966. Biosynthesis of the peptidoglycan of bacterial cell walls. I. Utilization of uridine diphosphate acetylmuramyl pentapeptide and uridine diphosphate acetylglucosamine for peptidoglycan synthesis by particulate enzymes from *Staphylococcus aureus* and *Micrococcus lysodeikticus*. Arch Biochem Biophys **116**:487-515.

5. Archibald, A. R., I. C. Hancock, and C. R. Harwood. (ed.). 1993. Cell wall structure, synthesis, and turnover. American Society for Microbiology, Washington, D. C.

6. Archibald, A. R., J. J. Armstrong, J. Baddiley, and J. B. Hay. 1961. Teichoic acids and the structure of bacterial walls. Nature **191**:570-2.

7. Bertsche, U., T. Kast, B. Wolf, C. Fraipont, M. E. Aarsman, K. Kannenberg, M. von Rechenberg, M. Nguyen-Disteche, T. den Blaauwen, J. V. Holtje, and W. Vollmer. 2006. Interaction between two murein (peptidoglycan) synthases, PBP3 and PBP1B, in *Escherichia coli*. Mol Microbiol **61**:675-90.

8. Bhavsar, A. P., X. Zhao, and E. D. Brown. 2001. Development and characterization

of a xylose-dependent system for expression of cloned genes in *Bacillus subtilis*: conditional complementation of a teichoic acid mutant. Appl Environ Microbiol **67**:403-10.

9. Buchanan, C. E., and M. L. Ling. 1992. Isolation and sequence analysis of dacB, which encodes a sporulation-specific penicillin-binding protein in *Bacillus subtilis*. J Bacteriol **174**:1717-25.

10. Cabeen, M. T., and C. Jacobs-Wagner. 2005. Bacterial cell shape. Nat Rev Microbiol **3**:601-10.

11. Daniel, R. A., S. Drake, C. E. Buchanan, R. Scholle, and J. Errington. 1994. The *Bacillus subtilis* spoVD gene encodes a mother-cell-specific penicillin-binding protein required for spore morphogenesis. J Mol Biol **235**:209-20.

12. Daniel, R. A., and J. Errington. 2003. Control of cell morphogenesis in bacteria: two distinct ways to make a rod-shaped cell. Cell **113**:767-76.

13. Daniel, R. A., E. J. Harry, and J. Errington. 2000. Role of penicillin-binding protein PBP 2B in assembly and functioning of the division machinery of *Bacillus subtilis*. Mol Microbiol **35**:299-311.

14. Defeu Soufo, H. J., and P. L. Graumann. 2005. *Bacillus subtilis* actin-like protein MreB influences the positioning of the replication machinery and requires membrane proteins MreC/D and other actin-like proteins for proper localization. BMC Cell Biol **6**:10.

15. Denome, S. A., P. K. Elf, T. A. Henderson, D. E. Nelson, and K. D. Young. 1999. *Escherichia coli* mutants lacking all possible combinations of eight penicillin binding proteins: viability, characteristics, and implications for peptidoglycan synthesis. J Bacteriol **181**:3981-93.

16. Divakaruni, A. V., R. R. Loo, Y. Xie, J. A. Loo, and J. W. Gober. 2005. The cell-shape protein MreC interacts with extracytoplasmic proteins including cell wall assembly complexes in *Caulobacter crescentus*. Proc Natl Acad Sci U S A **102**:18602-7.

17. Formstone, A., and J. Errington. 2005. A magnesium-dependent mreB null mutant: implications for the role of mreB in *Bacillus subtilis*. Mol Microbiol **55**:1646-57.

18. Foster, S. J., and D. L. Popham (ed.). 2001. Structure and synthesis of cell wall, spore cortex, teichoic acids, S-layers, and capsules. American Society for Microbiology, Washingtion, D. C.

19. Gerrits, M. M., A. P. Godoy, E. J. Kuipers, M. L. Ribeiro, J. Stoof, S. Mendonca, A. H. van Vliet, J. Pedrazzoli, Jr., and J. G. Kusters. 2006. Multiple mutations in or adjacent to the conserved penicillin-binding protein motifs of the penicillin-binding protein 1A confer amoxicillin resistance to *Helicobacter pylori*. Helicobacter **11**:181-7.

20. Ghuysen, J. M. 1991. Serine beta-lactamases and penicillin-binding proteins. Annu Rev Microbiol **45**:37-67.

21. Goehring, N. W., M. D. Gonzalez, and J. Beckwith. 2006. Premature targeting of cell division proteins to midcell reveals hierarchies of protein interactions involved in divisome assembly. Mol Microbiol **61**:33-45.

22. Goehring, N. W., F. Gueiros-Filho, and J. Beckwith. 2005. Premature targeting of a cell division protein to midcell allows dissection of divisome assembly in *Escherichia coli*. Genes Dev **19**:127-37.

23. Goffin, C., and J. M. Ghuysen. 1998. Multimodular penicillin-binding proteins: an enigmatic family of orthologs and paralogs. Microbiol Mol Biol Rev **62**:1079-93.

24. Hakenbeck, R., and J. Coyette. 1998. Resistant penicillin-binding proteins. Cell Mol Life Sci **54**:332-40.

25. Harry, E. J., K. Pogliano, and R. Losick. 1995. Use of immunofluorescence to visualize cell-specific gene expression during sporulation in *Bacillus subtilis*. J Bacteriol **177**:3386-93.

26. Henriques, A. O., P. Glaser, P. J. Piggot, and C. P. Moran, Jr. 1998. Control of cell shape and elongation by the rodA gene in *Bacillus subtilis*. Mol Microbiol **28**:235-47.

27. Higashi, Y., J. L. Strominger, and C. C. Sweeley. 1967. Structure of a lipid

intermediate in cell wall peptidoglycan synthesis: a derivative of a C55 isoprenoid alcohol. Proc Natl Acad Sci U S A **57**:1878-84.

28. Ho, S. N., H. D. Hunt, R. M. Horton, J. K. Pullen, and L. R. Pease. 1989. Site-directed mutagenesis by overlap extension using the polymerase chain reaction. Gene **77**:51-9.

29. Hoskins, J., P. Matsushima, D. L. Mullen, J. Tang, G. Zhao, T. I. Meier, T. I. Nicas, and S. R. Jaskunas. 1999. Gene disruption studies of penicillin-binding proteins 1a, 1b, and 2a in *Streptococcus pneumoniae*. J Bacteriol **181**:6552-5.

30. Ishino, F., and M. Matsuhashi. 1981. Peptidoglycan synthetic enzyme activities of highly purified penicillin-binding protein 3 in *Escherichia coli*: a septum-forming reaction sequence. Biochem Biophys Res Commun **101**:905-11.

31. Jones, L. J., R. Carballido-Lopez, and J. Errington. 2001. Control of cell shape in bacteria: helical, actin-like filaments in *Bacillus subtilis*. Cell **104**:913-22.

32. Kruse, T., J. Bork-Jensen, and K. Gerdes. 2005. The morphogenetic MreBCD proteins of *Escherichia coli* form an essential membrane-bound complex. Mol Microbiol **55**:78-89.

3**3. Leighton, T. J., and R. H. Doi.** 1971. The stability of messenger ribonucleic acid during sporulation in *Bacillus subtilis*. J Biol Chem **246**:3189-95.

34. Macheboeuf, P., A. M. Di Guilmi, V. Job, T. Vernet, O. Dideberg, and A. Dessen. 2005. Active site restructuring regulates ligand recognition in class A penicillin-binding proteins. Proc Natl Acad Sci U S A **102**:577-82.

35. McPherson, D. C., A. Driks, and D. L. Popham. 2001. Two class A high-molecular-weight penicillin-binding proteins of *Bacillus subtilis* play redundant roles in sporulation. J Bacteriol **183**:6046-53.

36. McPherson, D. C., and D. L. Popham. 2003. Peptidoglycan synthesis in the absence of class A penicillin-binding proteins in *Bacillus subtilis*. J Bacteriol **185**:1423-31.

37. Meador-Parton, J., and D. L. Popham. 2000. Structural analysis of *Bacillus subtilis*

spore peptidoglycan during sporulation. J Bacteriol **182**:4491-9.

38. Meadow, P. M., J. S. Anderson, and J. L. Strominger. 1964. Enzymatic polymerization of UDP-acetylmuramyl.L-ala.D-glu.L-lys.D-ala.D-ala and UDP-acetylglucosamine by a particulate enzyme from *Staphylococcus aureus* and its inhibition by antibiotics. Biochem Biophys Res Commun **14**:382-7.

39. Murray, T., D. L. Popham, and P. Setlow. 1996. Identification and characterization of *pbpC*, the gene encoding *Bacillus subtilis* penicillin-binding protein 3. J Bacteriol **178**:6001-5.

40. Nicholas, R. A., S. Krings, J. Tomberg, G. Nicola, and C. Davies. 2003. Crystal structure of wild-type penicillin-binding protein 5 from *Escherichia coli*: implications for deacylation of the acyl-enzyme complex. J Biol Chem **278**:52826-33.

41. Pedersen, L. B., E. R. Angert, and P. Setlow. 1999. Septal localization of penicillin-binding protein 1 in *Bacillus subtilis*. J Bacteriol **181**:3201-11.

42. Pedersen, L. B., K. Ragkousi, T. J. Cammett, E. Melly, A. Sekowska, E. Schopick, T. Murray, and P. Setlow. 2000. Characterization of *ywhE*, which encodes a putative high-molecular-weight class A penicillin-binding protein in *Bacillus subtilis*. Gene **246**:187-96.

43. Pinho, M. G., H. de Lencastre, and A. Tomasz. 2000. Cloning, characterization, and inactivation of the gene *pbpC*, encoding penicillin-binding protein 3 of *Staphylococcus aureus*. J Bacteriol **182**:1074-9.

44. Pinho, M. G., and J. Errington. 2005. Recruitment of penicillin-binding protein PBP2 to the division site of *Staphylococcus aureus* is dependent on its transpeptidation substrates. Mol Microbiol **55**:799-807.

45. Pinho, M. G., S. R. Filipe, H. de Lencastre, and A. Tomasz. 2001. Complementation of the essential peptidoglycan transpeptidase function of penicillin-binding protein 2 (PBP2) by the drug resistance protein PBP2A in *Staphylococcus aureus*. J Bacteriol **183**:6525-31.

46. Popham, D. L., M. E. Gilmore, and P. Setlow. 1999. Roles of low-molecular-weight penicillin-binding proteins in *Bacillus subtilis* spore peptidoglycan synthesis and spore properties. J Bacteriol **181**:126-32.

47. Popham, D. L., J. Helin, C. E. Costello, and P. Setlow. 1996. Analysis of the peptidoglycan structure of *Bacillus subtilis* endospores. J Bacteriol **178**:6451-8.

48. Popham, D. L., and P. Setlow. 1995. Cloning, nucleotide sequence, and mutagenesis of the *Bacillus subtilis ponA* operon, which codes for penicillin-binding protein (PBP) 1 and a PBP-related factor. J Bacteriol **177**:326-35.

49. Popham, D. L., and P. Setlow. 1993. Cloning, nucleotide sequence, and regulation of the *Bacillus subtilis pbpF* gene, which codes for a putative class A high-molecular-weight penicillin-binding protein. J Bacteriol **175**:4870-6.

50. Popham, D. L., and P. Setlow. 1994. Cloning, nucleotide sequence, mutagenesis, and mapping of the *Bacillus subtilis pbpD* gene, which codes for penicillin-binding protein 4. J Bacteriol **176**:7197-205.

51. Popham, D. L., and P. Setlow. 1996. Phenotypes of *Bacillus subtilis* mutants lacking multiple class A high-molecular-weight penicillin-binding proteins. J Bacteriol **178**:2079-85.

52. Reeve, J. N., N. H. Mendelson, S. I. Coyne, L. L. Hallock, and R. M. Cole. 1973. Minicells of *Bacillus subtilis*. J Bacteriol **114**:860-73.

53. Rice, L. B., L. L. Carias, R. Hutton-Thomas, F. Sifaoui, L. Gutmann, and S. D. Rudin. 2001. Penicillin-binding protein 5 and expression of ampicillin resistance in *Enterococcus faecium*. Antimicrob Agents Chemother **45**:1480-6.

54. Rubio, A., and K. Pogliano. 2004. Septal localization of forespore membrane proteins during engulfment in *Bacillus subtilis*. Embo J **23**:1636-46.

55. Sauvage, E., F. Kerff, E. Fonze, R. Herman, B. Schoot, J. P. Marquette, Y. Taburet, D. Prevost, J. Dumas, G. Leonard, P. Stefanic, J. Coyette, and P. Charlier. 2002. The 2.4-A crystal structure of the penicillin-resistant penicillin-binding protein

PBP5fm from *Enterococcus faecium* in complex with benzylpenicillin. Cell Mol Life Sci **59**:1223-32.

56. Scheffers, D. J. 2005. Dynamic localization of penicillin-binding proteins during spore development in *Bacillus subtilis*. Microbiology **151**:999-1012.

57. Scheffers, D. J., and J. Errington. 2004. PBP1 is a component of the *Bacillus subtilis* cell division machinery. J Bacteriol **186**:5153-6.

58. Scheffers, D. J., L. J. Jones, and J. Errington. 2004. Several distinct localization patterns for penicillin-binding proteins in *Bacillus subtilis*. Mol Microbiol **51**:749-64.

59. Schiffer, G., and J. V. Holtje. 1999. Cloning and characterization of PBP 1C, a third member of the multimodular class A penicillin-binding proteins of *Escherichia coli*. J Biol Chem **274**:32031-9.

60. Schleifer, K. H., and O. Kandler. 1972. Peptidoglycan types of bacterial cell walls and their taxonomic implications. Bacteriol Rev **36**:407-77.

61. Smith, A. M., and K. P. Klugman. 2005. Amino acid mutations essential to production of an altered PBP 2X conferring high-level beta-lactam resistance in a clinical isolate of *Streptococcus pneumoniae*. Antimicrob Agents Chemother **49**:4622-7.

62. Sowell, M. O., and C. E. Buchanan. 1983. Changes in penicillin-binding proteins during sporulation of *Bacillus subtilis*. J Bacteriol **153**:1331-7.

63. Stewart, G. C. 2005. Taking shape: control of bacterial cell wall biosynthesis. Mol Microbiol **57**:1177-81.

64. Takasuga, A., H. Adachi, F. Ishino, M. Matsuhashi, T. Ohta, and H. Matsuzawa. 1988. Identification of the penicillin-binding active site of penicillin-binding protein 2 of *Escherichia coli*. J Biochem (Tokyo) **104**:822-6.

65. Terrak, M., T. K. Ghosh, J. van Heijenoort, J. Van Beeumen, M. Lampilas, J. Aszodi, J. A. Ayala, J. M. Ghuysen, and M. Nguyen-Disteche. 1999. The catalytic, glycosyl transferase and acyl transferase modules of the cell wall peptidoglycan-polymerizing penicillin-binding protein 1b of *Escherichia coli*. Mol

Microbiol **34**:350-64.

66. Tipper, D. J., and J. L. Strominger. 1965. Mechanism of action of penicillins: a proposal based on their structural similarity to acyl-D-alanyl-D-alanine. Proc Natl Acad Sci U S A **54**:1133-41.

67. Tiyanont, K., T. Doan, M. B. Lazarus, X. Fang, D. Z. Rudner, and S. Walker. 2006. Imaging peptidoglycan biosynthesis in *Bacillus subtilis* with fluorescent antibiotics. Proc Natl Acad Sci U S A **103**:11033-8.

68. Todd, J. A., A. N. Roberts, K. Johnstone, P. J. Piggot, G. Winter, and D. J. Ellar. 1986. Reduced heat resistance of mutant spores after cloning and mutagenesis of the *Bacillus subtilis* gene encoding penicillin-binding protein 5. J Bacteriol **167**:257-64.

69. van der Linden, M. P., L. de Haan, O. Dideberg, and W. Keck. 1994. Site-directed mutagenesis of proposed active-site residues of penicillin-binding protein 5 from *Escherichia coli*. Biochem J **303** (Pt 2):357-62.

70. van Heijenoort, Y., M. Gomez, M. Derrien, J. Ayala, and J. van Heijenoort. 1992. Membrane intermediates in the peptidoglycan metabolism of *Escherichia coli*: possible roles of PBP 1b and PBP 3. J Bacteriol **174**:3549-57.

71. Vicente, M., A. I. Rico, R. Martinez-Arteaga, and J. Mingorance. 2006. Septum enlightenment: assembly of bacterial division proteins. J Bacteriol **188**:19-27.

72. Wada, A., and H. Watanabe. 1998. Penicillin-binding protein 1 of *Staphylococcus aureus* is essential for growth. J Bacteriol **180**:2759-65.

73. Ward, J. B. 1973. The chain length of the glycans in bacterial cell walls. Biochem J **133**:395-8.

74. Wei, Y., T. Havasy, D. C. McPherson, and D. L. Popham. 2003. Rod shape determination by the *Bacillus subtilis* class B penicillin-binding proteins encoded by *pbpA* and *pbpH*. J Bacteriol **185**:4717-26.

75. Wei, Y., D. C. McPherson, and D. L. Popham. 2004. A mother cell-specific class B penicillin-binding protein, PBP4b, in *Bacillus subtilis*. J Bacteriol **186**:258-61.

76. Welzel, P. (ed.). 1993. Transglycosylase inhibition. Wiley-VCH Verlag GmbH & Co. KGaA, Weinheim.

77. Williams, J. D. 1999. Beta-lactamases and beta-lactamase inhibitors. Int J Antimicrob Agents 12 Suppl 1:S3-7; discussion S26-7.

78. Wu, J. J., R. Schuch, and P. J. Piggot. 1992. Characterization of a *Bacillus subtilis* sporulation operon that includes genes for an RNA polymerase sigma factor and for a putative DD-carboxypeptidase. J Bacteriol **174**:4885-92.

79. Wyke, A. W., J. B. Ward, M. V. Hayes, and N. A. Curtis. 1981. A role in vivo for penicillin-binding protein-4 of *Staphylococcus aureus*. Eur J Biochem **119**:389-93.

80. Yanouri, A., R. A. Daniel, J. Errington, and C. E. Buchanan. 1993. Cloning and sequencing of the cell division gene *pbpB*, which encodes penicillin-binding protein 2B in *Bacillus subtilis*. J Bacteriol **175**:7604-16.

81. Yousif, S. Y., J. K. Broome-Smith, and B. G. Spratt. 1985. Lysis of *Escherichia coli* by beta-lactam antibiotics: deletion analysis of the role of penicillin-binding proteins 1A and 1B. J Gen Microbiol **131**:2839-45.